Discovery of Small-Molecule Inhibitors of the PTK7/β-Catenin Interaction Targeting the Wnt Signaling Pathway in Colorectal Cancer

Laetitia Ganier, Stéphane Betzi, Carine Derviaux, Philippe Roche, Charlotte Dessaux, Christophe Muller, Laurent Hoffer, Xavier Morelli, Jean-Paul Borg

Discovery of small molecule inhibitors of the PTK7/β-catenin interaction targeting the Wnt signaling pathway in colorectal cancer

Laetitia Ganier[1,2], Stéphane Betzi[2,3], Carine Derviaux[3], Philippe Roche[2,3], Charlotte Dessaux[1], Christophe Muller[3,†], Laurent Hoffer[2,‡], Xavier Morelli[2,3],* and Jean-Paul Borg[1,4] *

[1]Aix Marseille Univ, CNRS, INSERM, Institut Paoli-Calmettes, CRCM, Equipe labellisée Ligue 'Cell polarity, Cell signaling and Cancer', Marseille, France

[2]Aix Marseille Univ, CNRS, INSERM, Institut Paoli-Calmettes, CRCM, team 'Integrative Structural and Chemical Biology', Marseille, France

[3]Aix Marseille Univ, CNRS, INSERM, Institut Paoli-Calmettes, CRCM, 'HiTS/IPCdd – High throughput screening platform', Marseille, France
[4] Institut Universitaire de France

ABSTRACT: Second cause of death due to cancer worldwide, colorectal cancer (CRC) is a major public health issue. The discovery of new therapeutic targets is thus essential. The pseudokinase PTK7 intervenes in the regulation of the Wnt/β-catenin pathway signaling, in part, through a kinase-domain dependent interaction with the β-catenin protein. PTK7 is overexpressed in CRC; an event associated with metastatic development and reduced survival of non-metastatic patient. In addition, numerous alterations have been identified in CRC inducing constitutive activation of Wnt/β-catenin pathway signaling through β-catenin accumulation. Thus,targeting PTK7/β-catenin interaction could be of interest for future drug development. We have developed a NanoBRET™ screening assay recapitulating the interaction between PTK7 and β-catenin to identify compounds able to disrupt this protein-protein interaction. A high-throughput screening allowed us to identify small molecule inhibitors targeting the Wnt pathway signaling and inducing anti-proliferative and anti-tumor effect *in vitro* in CRC cells harboring *β-catenin* or *APC* mutations. Thus, inhibition of the PTK7/β-catenin interaction could represent a new therapeutic strategy to inhibit cell growth dependent on Wnt signaling pathway. Moreover, despite a lack of enzymatic activity of its tyrosine kinase domain, targeting the PTK7 kinase domain-dependent functions appears to be of interest for further therapeutic development.

INTRODUCTION

Colorectal cancer (CRC) is the second deadliest cancer worldwide with almost 900.000 deaths estimated in 2018 by the GLOBOCAN 2018[1]. Survival of patients with metastatic CRC has significantly improved over the past two decades with an average overall survival of 30 months. This is mainly due to the use of chemotherapies such as oxaliplatin and irinotecan but also to the introduction of targeted therapies. However none of them has shown survival improvement in the adjuvant setting[2,3]. Discovery of new therapeutic targets via a better characterization of molecular key players of CRC is thus essential.

CRC cells frequently reactivate the Wnt pathway involved in the establishment and maintenance of cell polarity, fundamental for embryonic development of vertebrates and invertebrates. The Wnt pathway is classically divided into two pathways: the canonical pathway also called Wnt/β-catenin, and the non-canonical pathway independent of β-catenin, itself subdivided into two pathways, Wnt/Planar Cell Polarity and Wnt/Ca^{2+} pathways[4].

Reactivation of the Wnt pathway in cancer cells plays an important role at different steps of the tumoral process such as auto-renewal of cancer stem cells, tumorigenesis, metastatic dissemination and resistance to treatments[5]. Alterations of multiple actors of the Wnt signaling, including *Adenomatous Polyposis Coli* (APC), β-catenin or Axin, are found in 93% of CRC[6]. Most of these alterations induce constitutive activation of Wnt/β-catenin pathway signaling through β-catenin accumulation and transcription of target genes involved in tumorigenesis such as *c-MYC* or *CCND1*[7,8]. Despite increasing attention paid to Wnt/β-catenin pathway in therapeutic development, few molecules have reached clinical trial to date[9].

The tyrosine kinase receptor PTK7 is a cell surface component of the Wnt pathway[10]. PTK7 was first identified in human normal melanocytes and in colon carcinoma[11,12]. PTK7 is composed of seven extracellular immunoglobulin domains, a transmembrane region and an intracellular tyrosine kinase domain.

However, its kinase domain lacks enzymatic activity and therefore this receptor is considered as a pseudokinase[13]. In retrospective studies, PTK7 was found overexpressed in CRC, an event associated with metastatic development, reduced metastases-free survival of non-metastatic patients, and resistance to chemotherapy. PTK7 has pro-migratory and pro-metastatic functions *in vitro* and *in vivo*. However, the mechanisms behind are not well understood yet[14,15]. PTK7 appears to be a promising new therapeutic target. A unique therapeutic approach has so far reached the clinical phases and consists in an antibody-drug conjugate (ADC) targeting tumor cells overexpressing PTK7[16]. Here, PTK7 behaves as a cell surface antigen enabling the destruction of PTK7-positive cancer cells. Development of alternative strategies to ADC through the development of chemical compounds targeting the PTK7 kinase domain-dependent functions would be of great interest. Indeed, we and others have shown that the kinase domain is endowed with signaling functions despite lack of enzymatic activity[17–21]. The role of PTK7 in Wnt/β-catenin pathway has been demonstrated in several studies. Peradziryi *et al* have shown an inhibitory role of PTK7 on the Wnt/βcatenin signaling, which was confirmed in zebrafish[22,23].

However, two other studies including one from our group identified LRP6 and β-catenin as new partners of PTK7 and have correlated loss of PTK7 with inhibition of Wnt/β-catenin signaling[17,24]. We demonstrated that PTK7 binds to β-catenin using a yeast two hybrid assay. We showed that this direct interaction is mediated by the kinase domain of PTK7 and that it is required for β-catenin-dependent transcriptional events[17].

In this report, we have developed a NanoBRET™ screening assay which recapitulates the interaction between PTK7 and β-catenin *in cellulo* and is applicable for high throughput screening (HTS) of chemical compounds able to disrupt the PTK7/β-catenin interaction[25]. We used different strategies based on virtual screening[26], HTS of the 'Fr-PPIChem' library (10,314 compounds)[27] and repurposing of TCF/β-catenin inhibitors[28]. These strategies allowed us to identify PTK7/β-catenin small molecules inhibitors targeting Wnt pathway signaling in CRC cells as evidenced in cell-based NanoBRET™ and TopFlash/Luciferase reporter assays. These compounds exhibit an *in vitro* anti-proliferative and anti-tumor effect on CRC cells harboring *β-catenin* or *APC* mutations downstream of PTK7, showing the potential of PTK7/ β-catenin targeting for future drug development.

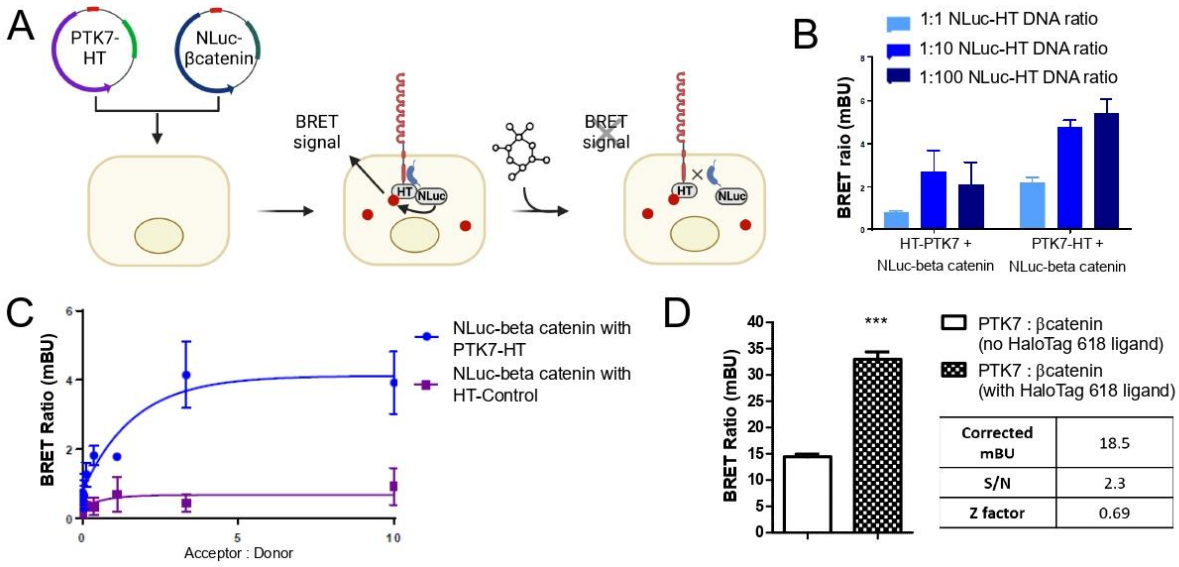

Figure 1. Development and validation of a NanoBRET assay monitoring PTK7/β-catenin interaction in living cells and optimization for high-throughput screening. (A) Scheme illustrating the proximity-based NanoBRET assay. PTK7-HT (HaloTag) and NL (NanoLuc)-β-catenin expressing plasmids are transfected in HEK293T cells. Cells are incubated with HaloTag 618 ligand (red circle) and Furimazine (Nano-Luciferase substrate) is added to allow generation of a BRET signal. (B) N- and C-terminal HT fusions to PTK7 with NL-β-catenin were tested at three donor to acceptor ratios. (C) Donor Saturation Assay (DSA) showing specificity for the detection of the interaction between NL-β-catenin and PTK7-HT. Cells were transfected with constant amount of NL donor DNA and paired with increasing amounts of acceptor DNA to obtain increasing amounts of Acceptor-to-Donor (A/D) ratios (blue line). The negative control is an unfused HaloTag® protein used as mock acceptor (purple line). (D) Optimization of the NanoBRET PTK7/β-catenin interaction assay for HTS. HEK293T cells expressing PTK7-HT and NL-β-catenin were plated in a 384-well plate with HaloTag 618 ligand to generate a positive BRET signal or DMSO as negative control. Data represents 176 (positive control) and 16 (negative control) wells, with mean ± SD (t test, ***p<0.001). Donor-to-acceptor ratios in positive and negative controls were used to calculate the Signal-to-Noise ratio (S/N). The Z-factor is defined with means (μ) and standard deviations (σ) of both positive (p) and negative (n) controls.. A S/N ratio >2 and a Z-factor value between 0.5 and 1 are suitable for HTS.

RESULTS AND DISCUSSION

Development and validation of a NanoBRET™ assay monitoring PTK7/β-catenin interaction in living cells and optimization for HTS. We developed a NanoBRET™ assay to confirm the PTK7/β-catenin interaction and to identify small molecular modulators of the complex in a cellular environment. This technology enables sensitive and reproducible detection of protein interactions *in cellulo* and is applicable for drug screening[29]. The NanoBRET™ system is a proximity-based assay that can detect protein interactions by measuring energy transfer from a bioluminescent NanoLuc® (NL) fusion protein as an energy donor to a fluorescently labeled HaloTag® (HT) fusion protein as an energy acceptor (**Figure 1A**)[25]. Initial development of the PTK7/β-catenin NanoBRET™ assay was performed with the assistance of Promega Company. Different constructs were generated by appending the HT acceptor tag to PTK7 in N- or C-terminal. The different combinations were tested and PTK7-HT + NL-β-catenin were identified as the optimal pair which yielded an optimal donor to acceptor BRET ratio at 1:10 (**Figure 1B**). Donor Saturation Assay (DSA) showed excellent specificity and assay window. The specific interaction generated a hyperbolic curve indicative of a specific BRET interaction detection. Interaction with an unfused HT protein alone as negative control generated a much weaker linear ratio (**Figure 1C**). Following this, an acceptor to donor ratio of 10:1 was used for further assay validation and screening as it lays within the ideal dynamic range for the detection of PTK7/β-catenin interaction changes. To validate the NanoBRET™ assay for HTS, HEK293 cells transiently transfected with PTK7-HT and NL-β-catenin plasmids, were plated in 384-well plates. The HaloTag 618 ligand was added to generate a positive control signal whereas DMSO alone was added for the negative control signal. The assay statistics evaluation exhibited a 0.69 Z'-factor value and a >2 signal to background ratio (**Figure 1D**). Taken together, these values confirmed that we were able to develop a specific and sensitive PTK7/β-catenin NanoBRET™ interaction assay compatible with high-throughput screening applications.

Use of different approaches to identify small-molecule inhibitors of the PTK7/β-catenin interaction. To identify chemical compounds that inhibit the PTK7/β-catenin protein-protein interaction (PPI), we developed a multi-screening strategy based on our newly developed NanoBRET™ assay that combined virtual screening, HTS and repurposing of drug in development as summarized in **Figure 2A**.

In a first approach, we took advantage of the recently published X-ray structure of unliganded inactive PTK7 kinase domain to perform an *in silico* screening of the Fr-PPIChem library (10,314 compounds). This library has been designed to contain potential protein-protein interaction inhibitor (iPPI) compounds[13,27]. This structure was used as a starting template to identify potential direct binders of PTK7. The experimental approach was based on a strategy described previously[26] and combines three robust computational approaches: Molecular Dynamics (MD) simulations, molecular docking methods, and pharmacophore filtering. The analysis of the MD trajectory of PTK7 protein identified conformations with putative larger druggable pockets that might be able to interact with small molecule compounds (**Figure S1A**). High-throughput molecular docking of the Fr-PPIChem library using PLANTS[30] and MOE (https://www.chemcomp.com/) led to the selection of the 200 best ligands (consensus scoring strategy). Finally, pharmacophore filtering using LigandScout[31], led to the selection of 92 prioritized compounds that were tested (**Figure S1B**).

Second, we performed an unbiased screening of the Fr-PPIChem library that could identify also β-catenin binders with a risk of loss of specificity. Indeed, β-catenin is the target of small molecule ligands[28] and contains central armadillo repeats responsible for binding with most of its partners including the transcription factors Tcf/Lef, APC and E-cadherin[28].

Third, we hypothesized that small molecule inhibitors of the β-catenin/Tcf4 interaction already in development could also block the PTK7/β-catenin interaction and serve as a basis for future optimization of the specificity. We selected some β-catenin/Tcf4 inhibitors with different specificity profiles towards Tcf4 (**Table S1**).

In the end, a total of 10,413 compounds selected from these three complementary strategies were evaluated using our optimized PTK7/β-catenin NanoBRET™ assay. From this HTS campaign, 3 compounds were identified as inhibitor hits from the *in silico* approach with IC_{50} values ranging from 15 to 40μM (**Figure 2B**) and 4 additional compounds from the random screening of the Fr-PPIChem library with IC_{50} values ranging from 5 to 10μM (**Figure 2C**). Interestingly, we could not identify compounds among the β-catenin/TCF4 inhibitors having inhibitory effect on the PTK7/β-catenin interaction (**Table S1**). This observation suggests a different binding site of PTK7 to β-catenin compared to Tcf4, APC or E-cadherin.

We confirmed hit compounds selectivity by performing a NanoBRET™ assay on another optimized control pair of vectors designed to measure the interaction between p53 and MDM2 (**Figure S2**). All compounds exhibit significant selectivity for PTK7/β-catenin over p53/MDM2 interaction (>5-fold). Compound 04967 exhibited the best inhibitory potential on the PTK7/β-catenin interaction with a 5.6 μM IC_{50}, as well as the highest selectivity ratio versus p53/MDM2 interaction with a 28.2 value (**Figure 2D**). Overall, the NanoBRET™ HTS campaign allowed the identification of seven hits (**Figure E-F**) inhibiting the PTK7/β-catenin interaction with micromolar range potency and good selectivity versus an irrelevant complex.

SAR-by-catalog resulting in the identification of PTK7/β-catenin inhibitors targeting Wnt pathway signaling in CRC cells. In order to overcome potential false positive and identify compounds with lower IC_{50}, we

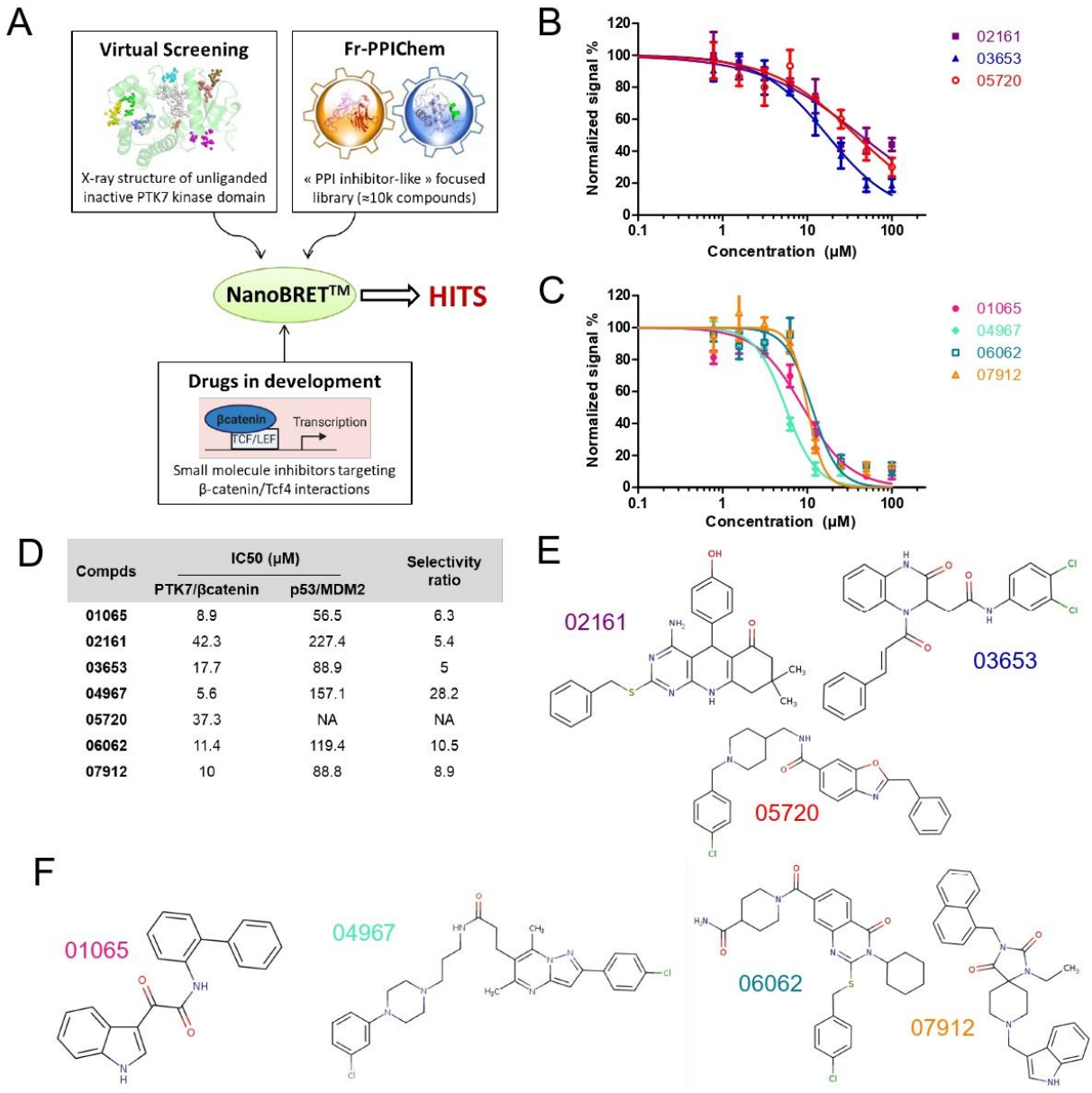

Compds	IC50 (μM)		Selectivity ratio
	PTK7/βcatenin	p53/MDM2	
01065	8.9	56.5	6.3
02161	42.3	227.4	5.4
03653	17.7	88.9	5
04967	5.6	157.1	28.2
05720	37.3	NA	NA
06062	11.4	119.4	10.5
07912	10	88.8	8.9

Figure 2. Use of different approaches to identify small-molecule inhibitors of the PTK7/β-catenin interaction. (A) Illustration of the different strategies used to identify hits: virtual screening, random screening and repurposing of drugs in development. (B-C) BRET signal in transiently transfected HEK293 cells with PTK7-HT and NL-β-catenin plasmids incubated overnight with increasing concentrations of compounds. Values are mean ± SD, n=3. NanoBRET IC_{50} assays allow the identification of 3 hits from the virtual screening strategy (B) and 4 hits from the Fr-PPIChem HTS (C). (D) Inhibitor selectivity of small molecule PTK7/β-catenin inhibitors over p53/MDM2 interaction determined by NanoBRET™. (E-F) Structures of PTK7/βcatenin inhibitors identify from the virtual screening (E) and the Fr-PPIChem HTS (F).

performed a structure-activity relationship study by purchasing commercially available compounds related to our hits (SAR-by-catalog). We ordered 5 to 13 analogs for each of our 7 compounds and NanoBRET™ IC_{50} assays were performed. Only 2 series of derivatives exhibited clear structure activity relationships (modulations of the compound scaffold affect the IC_{50}) confirming a specific inhibition of the complex (refer to **Table S2** for more details regarding the 2D chemical structures and IC_{50} information for all analogs). The first series includes 01065 identified from the Fr-PPIChem library and two of its analogs: 20269 and 20274 (**Figure 3A**). The second includes 03653 identified from the *in silico* screening on PTK7 X-ray structure and two of its analogs: 20278 and 20279 (**Figure 3B**). Thus, we can hypothesize that this series binds to PTK7. These results prompted us to further investigate how these molecules could modulate Wnt pathway signaling and confirm their potential as molecular probes of the PTK7/β-catenin interaction in cells.

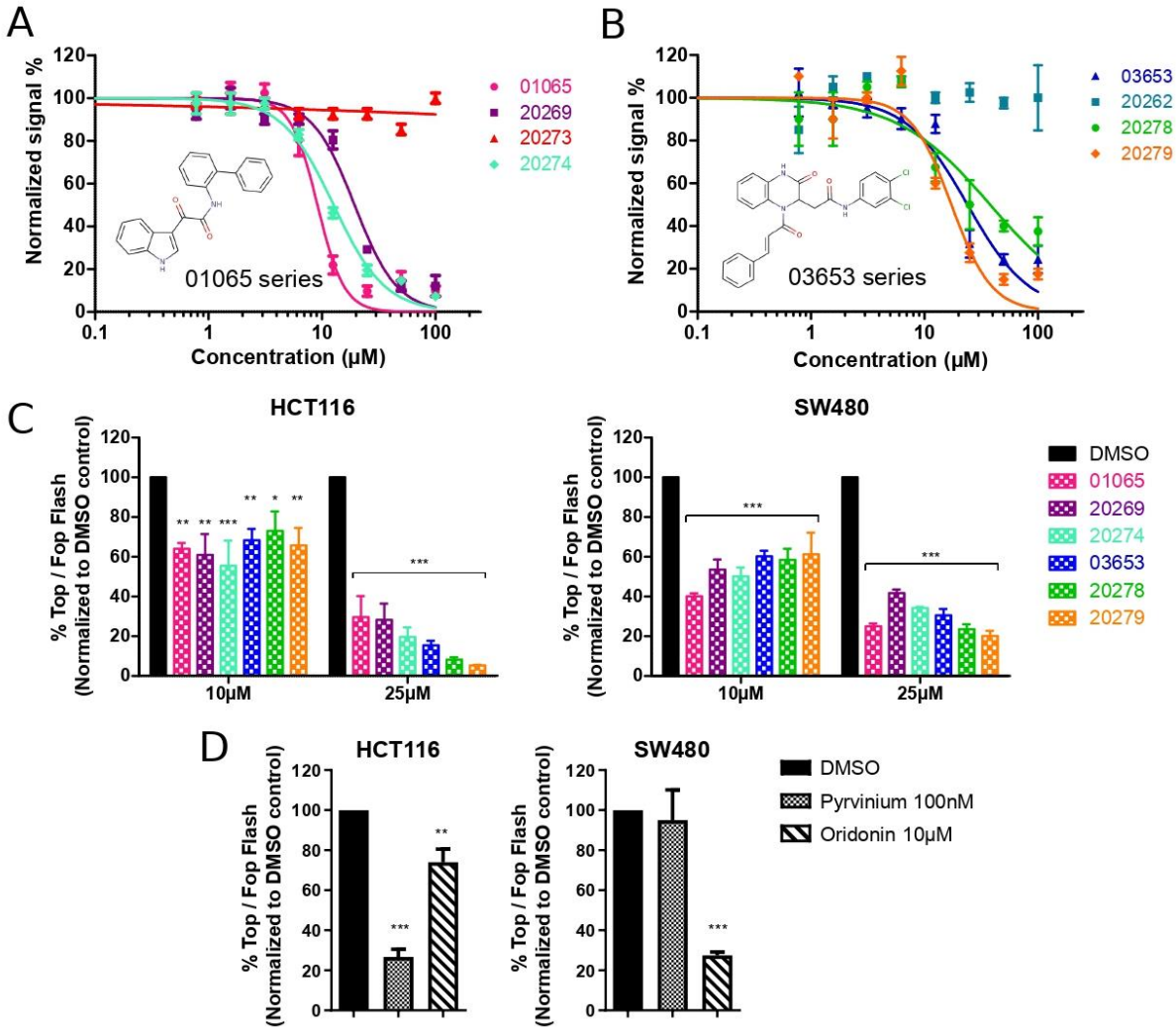

Figure 3. Use of SAR-by-catalog resulted in the identification of PTK7/β-catenin inhibitors targeting the Wnt signaling pathway in CRC cells. (A-B) BRET signal in transiently transfected HEK293 cells incubated with increasing concentrations of hit analogs. Values are mean ± SD, n=3. NanoBRET IC_{50} assays on the 55 analogs allow identification of active analogs only for the 01065 (A) and 03653 (B) hits. (C-D) Effect of the different compounds on WNT signaling pathway. HCT116 and SW480 were incubated with PTK7-β-catenin inhibitors at 10 and 25μM (C) and Pyrvinium (100nM) or Oridonin at (10μM) as positive controls (D). Wnt signaling activity was measured using the TopFlash/Luciferase reporter assay normalized with FOP activity and expressed as percentage of control cells treated with DMSO. Results are expressed as mean of 3 independent experiments ± SD and *P* values are derived from two-way Anova (*p < 0.05; **p <0.01; ***p < 0.001).

As mentioned, the role of PTK7 in the Wnt/β-catenin signaling pathway is cell context dependent[17,22–24]. To evaluate PTK7 involvement in the Wnt/β-catenin signaling in CRC, we used two colorectal cancer cell lines (HCT116 and SW480) with different mutational status. HCT116 cells are heterozygous for *β-catenin* with a mutant allele bearing a mutation of a serine involved in the negative regulation of β-catenin following phosphorylation by GSK3[32]. SW480 cells are APC^{mt} resulting in a C-terminal truncated protein lacking the β-catenin binding domain[33]. Both mutations induce a constitutive activation of the Wnt/β-catenin pathway signaling in HCT116 and SW480.

Firstly, these two CRC cell lines were transfected with a potent siRNA against PTK7 (**Figure S3A**) and effect on the Wnt/β-catenin signaling was evaluated using a β-catenin bioluminescent reporter assay (TOPflash normalized with FOPflash). We observed a significant inhibition in the transactivating activity of β-catenin following PTK7 down-regulation in the two cell lines (**Figure S3B**). These results are in line with those of Puppo *et al.*[17] and suggest an inhibitory role of PTK7 on Wnt/β-catenin signaling independently of *β-catenin* or *APC* mutations.

We thus moved to the biological validation of our two series of compounds. CRC cells were treated overnight with all compounds at 10 and 25μM and activity on Wnt signaling was evaluated with the β-catenin bioluminescent reporter assay. All compounds significantly decreased the transactivating activity of β-catenin in HCT116 and SW480

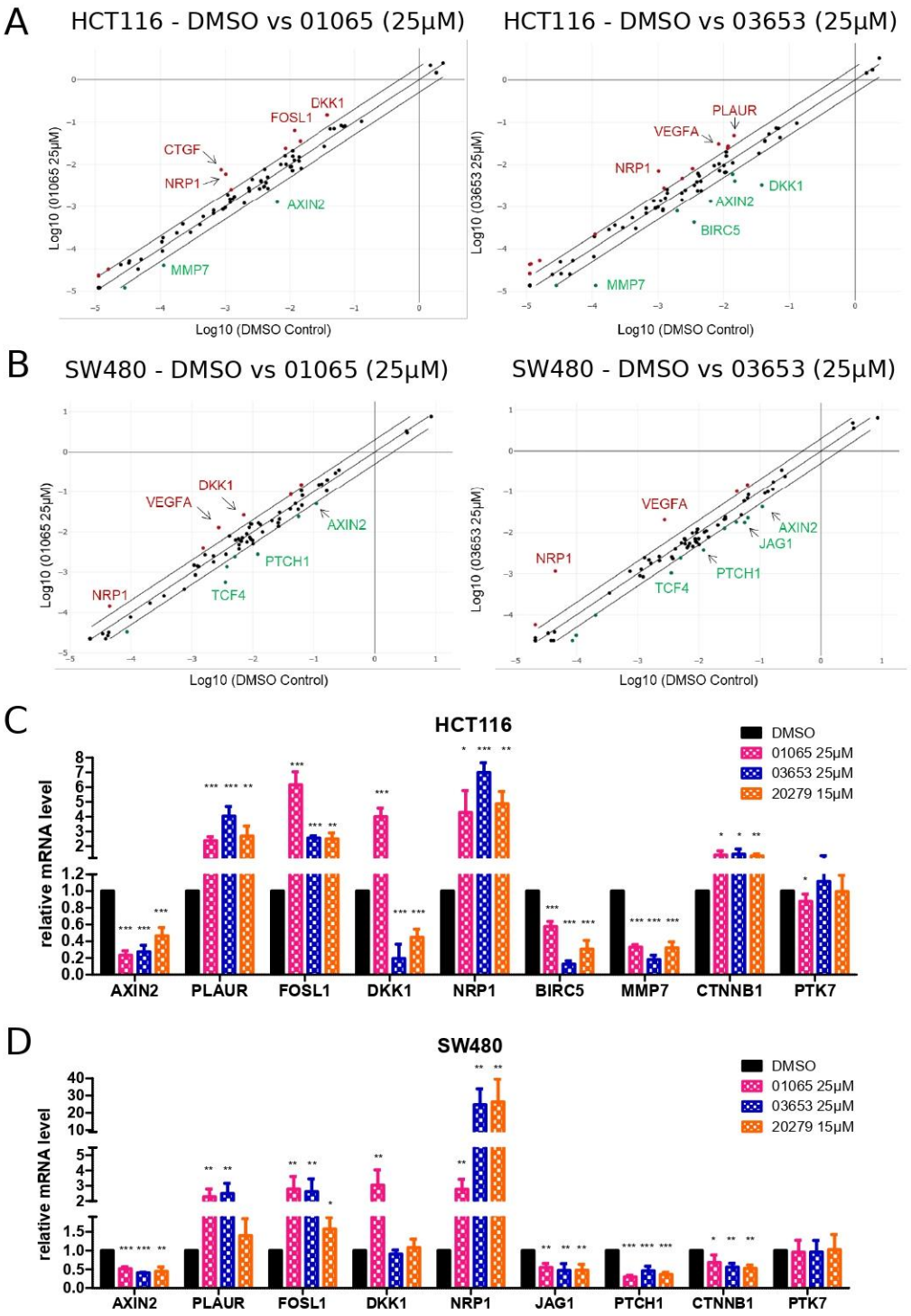

Figure 4. PTK7/β-catenin inhibitors modulate Wnt signaling target genes expression in CRC cells. (A-B) Effects of PTK7/β-catenin inhibitors on Wnt signaling target genes expression profiles in HCT116 (A) and SW480 (B) cells. Cells were treated 24h with 01065 and 03653 at 25µM. The expression change of the 84 genes in samples and control groups was revealed by real-time PCR based array analysis. Scatter plots graph the $\log_{10}$ of the expression level of each gene in the sample group versus the corresponding value in the control group (DMSO). The central line indicates fold changes of 1, or no change. The external lines indicate a fold-change threshold of 2. The red and green dots stand for up-regulated and down-regulated genes respectively. (C-D) Validation of selected candidate genes with classical RT-qPCR in HCT116 (C) and SW480 (D). Cells were treated with compounds 01065 and 03653 at 25µM or 20279 at 15µM. Data show relative mRNA levels of candidate genes in sample groups against DMSO control group. Results are expressed as mean of 3 independent experiments ± SD and *P* values are derived from t-tests (*p < 0.05; **p <0.01; ***p < 0.001).

in a dose-dependent manner (**Figure 3C**). As part of the biological validation, an analog from the 03653 series not selected in NanoBRET™ (compound 20262) had no effect on Wnt signaling activation in both cell lines at 25µM (**Figure S3C**). We also evaluated two known inhibitors of the Wnt signaling pathway as positive controls: Pyrvinium, which acts through casein kinase 1α activation[34] and Oridonin through inhibition of TCF/β-catenin interaction[28]. Interestingly, we observed a context-dependent effect of these compounds with Pyrvinium being effective on HCT116 only at 100nM and Oridonin being more effective on SW480 at 10µM (**Figure 3D**). Considering the above results, we conclude that PTK7/β-catenin inhibition with small molecules attenuate Wnt signaling activation in CRC cells independently of *β-catenin* or *APC* mutations compared to known inhibitors of the Wnt pathway signaling.

PTK7/β-catenin inhibition with small molecules modulates Wnt signaling target genes expression in CRC cells. To analyze the effect of our compounds on Wnt signaling pathway, we used a RT² profiler PCR array to analyze the expression of 84-Wnt related target genes following treatment of CRC cells. These 84 genes are listed in **Table S3** with their main associated functions as for example cell migration or cell cycle regulation. HCT116 and SW480 cells were treated with the two hits, 01065 and 03653, at 25µM for gene expression analysis. Analogs were not tested in the preliminary screening based on the assumption that they should have a similar mechanism than their related compound. Results are presented on scatter plots (**Figure 4A-B**). Gene expression changes are beyond the boundary lines with a fold-change threshold of 2 and are represented in red dots for up-regulated genes or green dots for down-regulated genes. The RT² screening led to the identification of Wnt target genes differentially regulated in a same way in all conditions such as *AXIN2* but also genes modulated in a cell line- or compound-dependent fashion as for *MMP7* downregulated only in HCT116 or *DKK1* upregulated in both cell lines following treatment with compound 01065 only.

We then validated selected genes candidate from gene profiling analysis with classical RT-qPCR in HCT116 (**Figure 4C**) and SW480 (**Figure 4D**) cells. During the validation study, only the 20279 analog appeared to be more efficient than its parent compound and exhibited similar effects at 15µM to its parent compound (03653) at 25µM. We could confirm the significant reduction in *AXIN2* mRNA level in HCT116 and SW480. AXIN2 is a well-characterized target of misregulated β-catenin responsive transcription that acts as a feedback inhibitor to impede the activity of Wnt signaling pathway[35]. The three compounds also induce a significant upregulation in *PLAUR*, *FOSL1* and *NRP1* mRNA levels in both cell lines. Interestingly, a previous study has shown that siRNA-mediated silencing of β-catenin increased PLAUR expression at the mRNA and protein levels in SW480 cells which is consistent with our results[36]. NRP1 is strongly upregulated especially in SW480 treated with 03653 and 20279 with a fold change > 20. Interestingly, NRP1 was shown to have differential pro-tumoral *vs.* anti-tumoral effects depending on the type of cancer and the mutational status of *KRAS*. Inhibition of NRP1 expression in cells containing dominant active *KRAS*^{mt} caused increased cell viability and tumor growth[37]. As HCT116 and SW480 are both *KRAS*^{mt}, NRP1 upregulation led by 01065, 03653 and 20279 could theoretically reduce tumor growth. The compound 01065 only induces upregulation of *DDK1* mRNA encoding a secreted inhibitor of Wnt signaling, in both cell lines. Other chemical compounds, such as HDAC inhibitors, have been shown to upregulate DKK1 in colon cancer initiating cells and lead to cell cycle arrest and apoptosis[38]. Finally, other genes are specifically modulated in one cell line with all compounds tested. This includes down-regulation of *BIRC5* (survivin) and *MMP7* in HCT116, and *JAG1* and *PTCH1* in SW480. All these genes play crucial roles in cancer progression and particularly cell proliferation and cell survival so their down-regulation should promote anti-tumorigenic functions. Apart from Wnt target genes, no major effect of the compounds was evidenced on *PTK7* mRNA expression. However, *β-catenin* mRNA levels were down-regulated in SW480 cells. In this cell line, β-catenin cannot be degraded due to APC mutation and, in regards with Wnt/β-catenin signaling inhibition following compounds treatment, *β-catenin* mRNA down-regulation could be part of a transcriptomic negative feedback to reduce β-catenin protein level available in cells. In HCT116, *β-catenin* mRNA levels were slightly up-regulated but are not biologically significant as fold-changes are <2.

Altogether, these data show that PTK7/β-catenin inhibitors induce differential expression of Wnt signaling target genes associated with cell proliferation, cell survival and migration.

PTK7/β-catenin inhibitors impair proliferation and anchorage-independent cell growth. To investigate the antiproliferative properties of 01065, 03653 and 20279 *in cellulo*, we performed Alamar Blue assays on HCT116 and SW480 treated cells with increasing concentrations of compounds. All tested compounds exerted dose-dependent antiproliferative effects against CRC cells, compound 20279 being the most active in accordance with previous results (**Figure 5A – Table1**). We also evaluated the specificity over CRC cells by performing this assay on primary Mouse Embryonic Fibroblasts (MEFs) expressing PTK7. At a dose inducing maximum antiproliferative properties on CRC cells (30µM for 01065 and 03653 and 15µM for 20279); weak effect was observed on MEFs (**Figure 5A – Table1**).

Table 1. Table recapitulating IC_{50} values (concentration of compounds exhibiting 50% cell viability) in HCT116, SW480 and MEFs.

IC50 (µM)	01065	03653	20279
HCT116	19.6 ± 0.59	20.1 ± 1.7	11.3 ± 0.25
SW480	21.3 ± 0.84	19.6 ± 0.73	10.7 ± 0.30
MEF	41.0 ± 4.95	46.3 ± 4.77	21.2 ± 1.32

To further validate the effect of PTK7/β-catenin inhibitors we also performed *in vitro* soft agar colony formation assays, considered as the most stringent test for the detection of anchorage-independent tumor cell growth. The compounds 01065, 03653 and 20279 induced 52%, 46% and 40%

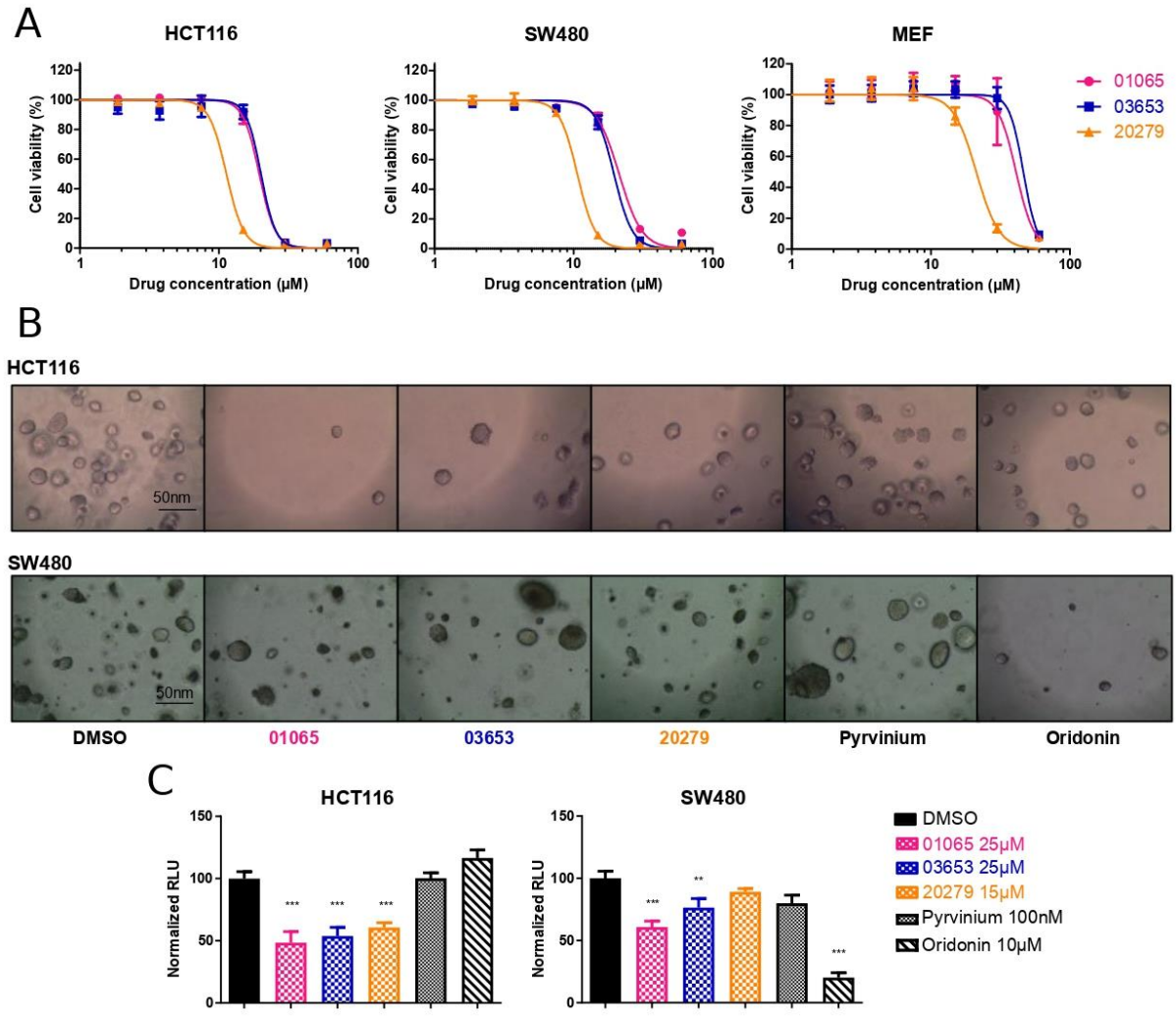

Figure 5. PTK7/β-catenin inhibitors impair anchorage-independent cell growth and proliferation. (A) Impact of PTK7/β-catenin inhibitors on HCT116, SW480 and MEFs viability *in vitro*. Cells were incubated with increasing concentration of compounds. Cell viability was assessed by Alamar Blue assay and expressed as percentage of control cells treated with DMSO. Points represent mean of 3 independent experiment and bars are SD. (B-C) Soft agar colony formation assays in HCT116 and SW480 after treatment with DMSO, PTK7/β-catenin inhibitors, pyrvinium or oridonin. (B) Representative images and (C) Bar graphs indicating luciferase activities expressed in relative light units (RLUs), relative to activities measured in DMSO control. Results are expressed as mean of 2 independent experiments ± SD and *P* values are derived from one-way Anova (**p <0.01; ***p < 0.001).

decrease in the growth of HCTT116 and 39%, 24% and 11% in SW480 respectively (**Figures 5B-C**). Among the two positive controls validated previously (Figure 3D) only oridonin appeared to strongly decrease cell growth of SW480 (80%) and none of them had effect on HCT116. We also excluded a potential effect of compounds cytotoxicity by performing a cell viability assay after treatment with the different compounds (**Figure S4**). Altogether, PTK7/β-catenin inhibitors demonstrate antiproliferative activity with highest selectivity over CRC cells, and inhibition of anchorage-independent cell growth in both HCT116 and SW480.

PTK7/β-catenin inhibitors cause cell cycle arrest of CRC cells. Wnt/β-catenin signaling is well known to promote cell proliferation through transcriptional upregulation of target genes involved in cell cycle progression. Another evidence of a relation between the cell cycle and Wnt signaling comes from the observations that β-catenin protein levels and Wnt/β-catenin signaling oscillate during the cell cycle[39,40]. Consistently with our previous findings, we investigated deeper the antiproliferative effect of our compounds. We performed a cell cycle distribution analysis based on a standard flow cytometry method by staining DNA with propidium iodide (PI). Interestingly, both 01065 and 03653 series induced an obvious cell cycle arrest through distinct mechanisms. On the one hand, compound 01065 increased the percentage of HCT116 and SW480 cells in S phase with subsequent decrease in G0/G1 phases suggesting S phase arrest that inhibits cell cycle progression (**Figure 6A**). On the other hand, the 03653 series strongly increased the percentage of HCT116 cells in G0/G1 phases, more moderately in the case of SW480 cells,

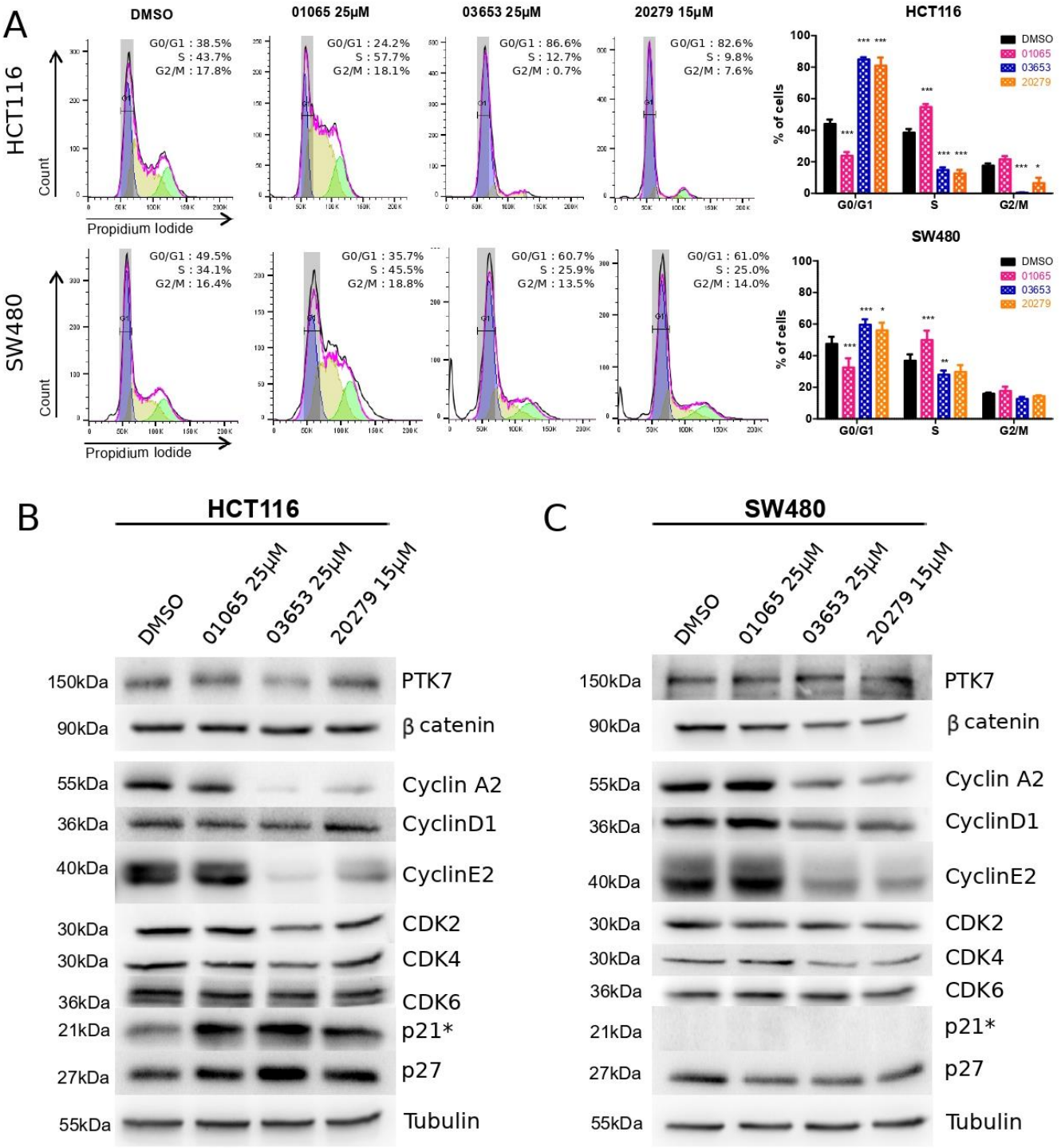

Figure 6. PTK7/β-catenin inhibitors cause cell cycle arrest in CRC cells. (A) Left: Cell cycle distribution of HCT116 and SW480 measured by propidium iodide (PI) staining and analyzed for DNA content by flow cytometry after treatment with DMSO, 25µM of 01065 and 03653 or 15µM of 20279 for 24hours. Right panel: Cell cycle distribution is represented as histogram of the percentage of cells in G0/G1, S or G2/M phase. Results are expressed as mean of 3 independent experiments ± SD and *P* values are derived from two-way Anova (*p < 0.05; **p <0.01; ***p < 0.001). (B-C) Total cell lysates were extracted from HCT116 (B) and SW480 (C) cells to examine the expression levels of PTK7, βcatenin and key proteins involved in cell cycle regulation by western analysis. *To note p53 regulates p21 expression but while HCT116 are $p53^{wt}$, SW480 are $p53^{mt}$ rendering p53 inactive which explains why p21 is not expressed in this cell line[41,42].

suggesting also an inhibition of cell cycle progression (**Figure 6A**). We then determined the levels of key cell cycle regulators after drug treatment. In HCT116 cells, we could detect a significant increase in p21 and p27 protein levels for both series of compounds. The 03653 series also induced a strong decrease in CyclinA2 and CyclinE2 and a slight decrease in CDK proteins consistent with the observed cell cycle arrest (**Figures 6B and S5A**). Regarding SW480 cells, the results are less clear for the compound 01065 as no major regulation of cell cycle proteins was observed. However, we could detect a significant decrease in CyclinA2, CyclinD1, CyclinE2 and CDK4 but also in p27 with the 03653 series (**Figure 6C and S5B**).

Apart from cell cycle regulators, we could not detect any obvious alteration of PTK7 protein levels in both cell lines. Regarding β-catenin, the compounds did not reduce its protein level in HCT116 cells. One possible explanation for β-catenin responsive transcription inhibition could be an inhibition of β-catenin translocation into the nucleus *via* formation of E-cadherin/β-catenin complexes, for example, as it was shown in another study[43]. In SW480 cells, β-catenin protein levels are slightly decreased and only significantly upon treatment with compound 03653 (**Figures 6B-C**). However, this decrease could be due to *β-catenin* mRNA downregulation (**Figure 4C**).

Compound 01065 induced cell cycle arrest at S phase whereas 03653 and 20279 compounds induced cell cycle arrest at G0/G1 phases and consequently inhibited HCT116 and SW480 cell proliferation. However, HCT116 cells appear to be more sensitive to PTK7/β-catenin inhibitors than the SW480 cell line. One hypothesis could be that the β-catenin/PTK7 expression ratio is around 1 in SW480 while it is 0.5 in HCT116 (data not shown). Thus, an increase of PTK7/β-catenin complexes in SW480 could reduce compounds efficiency.

We also assessed if these compounds could induce cell apoptosis following cell cycle arrest. We performed a standard flow cytometry analysis by staining cells with Annexin V and propidium iodide (PI) 48 hours after treatment. However, we could not observe induction of cell apoptosis in the two cell lines suggesting that effect of our compounds is restricted to cell proliferation (**Figures S6A-B**). Association of these compounds with pro-apoptotic compounds could be of interest as concomitant growth arrest and apoptosis are required for effective targeted therapy[44,45].

In conclusion, we demonstrated that inhibition of the PTK7/β-catenin interaction is achievable with small molecules and could represent, in the future, a new therapeutic strategy to inhibit CRC cell growth dependent on Wnt signaling pathway. Additional studies will be required, particularly with regard to the potency of these compounds. These compounds also represent interesting molecular probes that can be used to target and modulate PTK7/βcatenin interaction and better understand this interaction in its pathways and in cancer development.

ASSOCIATED CONTENT

Supporting Information.

The Supporting Information is available free of charge via the internet at http://pubs.acs.org.

Cell lines and reagents; experimental methods for *in silico* structure-based screening, NanoBRET™ assay, TopFlash assay, cell viability assay, colony formation assay, RT² profiler PCR arrays, flow cytometry analysis and immunoblot analysis; *In silico* screening workflow, hit compounds selectivity, role of PTK7 on Wnt pathway signaling, western blot quantification, cell apoptosis analysis; List of 7 small molecule inhibitors targeting β-catenin/TCF4 interaction, List of 55 compounds to probe the SAR of hit compounds, List of 84 key genes responsive to Wnt signal transduction, primer sequences and antibodies.

AUTHOR INFORMATION

Corresponding Authors (*)

Xavier Morelli – Aix Marseille Univ, CNRS, INSERM, Institut Paoli-Calmettes, CRCM, team 'Integrative Structural and Chemical Biology', 13009 Marseille, France; Aix Marseille Univ, CNRS, INSERM, Institut Paoli-Calmettes, CRCM, 'HiTS/IPCdd – High throughput screening platform', 13009 Marseille, France; http://orcid.org/0000-0001-8101-7901
Email: xavier.morelli@inserm.fr

Jean-Paul Borg - Aix Marseille Univ, CNRS, INSERM, Institut Paoli-Calmettes, CRCM, Equipe labellisée Ligue 'Cell polarity, Cell signaling and Cancer', 13009 Marseille, France; Institut Universitaire de France; https://orcid.org/0000-0001-8418-3382
Email: jean-paul.borg@inserm.fr

Present Addresses

†Evotec – 195 Route d'Espagne, 31100 Toulouse, France
‡Drug Discovery Program, Ontario Institute for Cancer Research, Toronto, ON, Canada

Author Contributions

LG and SB designed the project, performed experiments, analyzed data and wrote the manuscript. C. Derviaux manages the High Throughput Screening platform HiTS/IPCdd and helped for the HTS screening. C. Dessaux performed the soft agar colony formation assay. CM performed the virtual screening. LH and PR performed the SAR-by-catalog analysis. JPB and XM supervised, analyzed, funded the project and wrote the manuscript. All authors have given approval to the final version of the manuscript.

Funding Sources

This work was funded by La Ligue Nationale Contre le Cancer (Label Ligue JPB, and PhD fellowship to LG), Fondation de France, Fondation pour la Recherche Médicale (4th year PhD fellowship to LG). JPB is a scholar of Institut Universitaire de France.

Notes

The authors declare no potential conflicts of interest.

ACKNOWLEDGMENT

The authors wish to thank the R&D department from Promega for the generation of the NanoBRET™ plasmids and validation of the assay. We thank Audrey Restouin for its expertise in the soft agar colony formation assay. We also thank La ligue Nationale Contre le Cancer and Fondation pour la Recherche Médicale for their support.

REFERENCES

(1) Bray, F.; Ferlay, J.; Soerjomataram, I.; Siegel, R. L.; Torre, L. A.; Jemal, A. Global Cancer Statistics 2018: GLOBOCAN Estimates of Incidence and Mortality Worldwide for 36 Cancers in 185 Countries. *CA: A Cancer Journal for Clinicians* **2018**, *68* (6), 394–424. https://doi.org/10.3322/caac.21492.

(2) Kuipers, E. J.; Grady, W. M.; Lieberman, D.; Seufferlein, T.; Sung, J. J.; Boelens, P. G.; van de Velde, C. J. H.; Watanabe, T. Colorectal Cancer. *Nat Rev Dis Primers* **2015**, *1*, 15065. https://doi.org/10.1038/nrdp.2015.65.

(3) Punt, C. J. A.; Koopman, M.; Vermeulen, L. From Tumour Heterogeneity to Advances in Precision Treatment of Colorectal Cancer. *Nat Rev Clin Oncol* **2017**, *14* (4), 235–246. https://doi.org/10.1038/nrclinonc.2016.171.

(4) Logan, C. Y.; Nusse, R. The Wnt Signaling Pathway in Development and Disease. *Annu Rev Cell Dev Biol* **2004**, *20*, 781–810. https://doi.org/10.1146/annurev.cellbio.20.010403.113126.

(5) MacDonald, B. T.; Tamai, K.; He, X. Wnt/Beta-Catenin Signaling: Components, Mechanisms, and Diseases. *Dev Cell* **2009**, *17* (1), 9–26. https://doi.org/10.1016/j.devcel.2009.06.016.

(6) Cancer Genome Atlas Network. Comprehensive Molecular Characterization of Human Colon and Rectal Cancer. *Nature* **2012**, *487* (7407), 330–337. https://doi.org/10.1038/nature11252.

(7) He, T. C.; Sparks, A. B.; Rago, C.; Hermeking, H.; Zawel, L.; da Costa, L. T.; Morin, P. J.; Vogelstein, B.; Kinzler, K. W. Identification of C-MYC as a Target of the APC Pathway. *Science* **1998**, *281* (5382), 1509–1512. https://doi.org/10.1126/science.281.5382.1509.

(8) Tetsu, O.; McCormick, F. Beta-Catenin Regulates Expression of Cyclin D1 in Colon Carcinoma Cells. *Nature* **1999**, *398* (6726), 422–426. https://doi.org/10.1038/18884.

(9) Cheng, X.; Xu, X.; Chen, D.; Zhao, F.; Wang, W. Therapeutic Potential of Targeting the Wnt/β-Catenin Signaling Pathway in Colorectal Cancer. *Biomed Pharmacother* **2019**, *110*, 473–481. https://doi.org/10.1016/j.biopha.2018.11.082.

(10) Lu, X.; Borchers, A. G. M.; Jolicoeur, C.; Rayburn, H.; Baker, J. C.; Tessier-Lavigne, M. PTK7/CCK-4 Is a Novel Regulator of Planar Cell Polarity in Vertebrates. *Nature* **2004**, *430* (6995), 93–98. https://doi.org/10.1038/nature02677.

(11) Lee, S. T.; Strunk, K. M.; Spritz, R. A. A Survey of Protein Tyrosine Kinase MRNAs Expressed in Normal Human Melanocytes. *Oncogene* **1993**, *8* (12), 3403–3410.

(12) Mossie, K.; Jallal, B.; Alves, F.; Sures, I.; Plowman, G. D.; Ullrich, A. Colon Carcinoma Kinase-4 Defines a New Subclass of the Receptor Tyrosine Kinase Family. *Oncogene* **1995**, *11* (10), 2179–2184.

(13) Sheetz, J. B.; Mathea, S.; Karvonen, H.; Malhotra, K.; Chatterjee, D.; Niininen, W.; Perttilä, R.; Preuss, F.; Suresh, K.; Stayrook, S. E.; Tsutsui, Y.; Radhakrishnan, R.; Ungureanu, D.; Knapp, S.; Lemmon, M. A. Structural Insights into Pseudokinase Domains of Receptor Tyrosine Kinases. *Mol. Cell* **2020**, *79* (3), 390-405.e7. https://doi.org/10.1016/j.molcel.2020.06.018.

(14) Lhoumeau, A.-C.; Martinez, S.; Boher, J.-M.; Monges, G.; Castellano, R.; Goubard, A.; Doremus, M.; Poizat, F.; Lelong, B.; de Chaisemartin, C.; Bardin, F.; Viens, P.; Raoul, J.-L.; Prebet, T.; Aurrand-Lions, M.; Borg, J.-P.; Gonçalves, A. Overexpression of the Promigratory and Prometastatic PTK7 Receptor Is Associated with an Adverse Clinical Outcome in Colorectal Cancer. *PLoS ONE* **2015**, *10* (5), e0123768. https://doi.org/10.1371/journal.pone.0123768.

(15) Meng, L.; Sefah, K.; O'Donoghue, M. B.; Zhu, G.; Shangguan, D.; Noorali, A.; Chen, Y.; Zhou, L.; Tan, W. Silencing of PTK7 in Colon Cancer Cells: Caspase-10-Dependent Apoptosis via Mitochondrial Pathway. *PLoS ONE* **2010**, *5* (11), e14018. https://doi.org/10.1371/journal.pone.0014018.

(16) Damelin, M.; Bankovich, A.; Bernstein, J.; Lucas, J.; Chen, L.; Williams, S.; Park, A.; Aguilar, J.; Ernstoff, E.; Charati, M.; Dushin, R.; Aujay, M.; Lee, C.; Ramoth, H.; Milton, M.; Hampl, J.; Lazetic, S.; Pulito, V.; Rosfjord, E.; Sun, Y.; King, L.; Barletta, F.; Betts, A.; Guffroy, M.; Falahatpisheh, H.; O'Donnell, C. J.; Stull, R.; Pysz, M.; Escarpe, P.; Liu, D.; Foord, O.; Gerber, H. P.; Sapra, P.; Dylla, S. J. A PTK7-Targeted Antibody-Drug Conjugate Reduces Tumor-Initiating Cells and Induces Sustained Tumor Regressions. *Sci Transl Med* **2017**, *9* (372). https://doi.org/10.1126/scitranslmed.aag2611.

(17) Puppo, F.; Thomé, V.; Lhoumeau, A.-C.; Cibois, M.; Gangar, A.; Lembo, F.; Belotti, E.; Marchetto, S.; Lécine, P.; Prébet, T.; Sebbagh, M.; Shin, W.-S.; Lee, S.-T.; Kodjabachian, L.; Borg, J.-P. Protein Tyrosine Kinase 7 Has a Conserved Role in Wnt/β-Catenin Canonical Signalling. *EMBO Rep.* **2011**, *12* (1), 43–49. https://doi.org/10.1038/embor.2010.185.

(18) Wehner, P.; Shnitsar, I.; Urlaub, H.; Borchers, A. RACK1 Is a Novel Interaction Partner of PTK7 That Is Required for Neural Tube Closure. *Development* **2011**, *138* (7), 1321–1327. https://doi.org/10.1242/dev.056291.

(19) Andreeva, A.; Lee, J.; Lohia, M.; Wu, X.; Macara, I. G.; Lu, X. PTK7-Src Signaling at Epithelial Cell Contacts Mediates Spatial Organization of Actomyosin and Planar Cell Polarity. *Dev Cell* **2014**, *29* (1), 20–33. https://doi.org/10.1016/j.devcel.2014.02.008.

(20) Na, H.-W.; Shin, W.-S.; Ludwig, A.; Lee, S.-T. The Cytosolic Domain of Protein-Tyrosine Kinase 7 (PTK7), Generated from Sequential Cleavage by a Disintegrin and Metalloprotease 17 (ADAM17) and γ-Secretase, Enhances Cell Proliferation and Migration in Colon Cancer Cells. *J Biol Chem* **2012**, *287* (30), 25001–25009. https://doi.org/10.1074/jbc.M112.348904.

(21) Golubkov, V. S.; Strongin, A. Y. Downstream Signaling and Genome-Wide Regulatory Effects of PTK7

Pseudokinase and Its Proteolytic Fragments in Cancer Cells. *Cell Commun Signal* **2014**, *12*, 15. https://doi.org/10.1186/1478-811X-12-15.

(22) Peradziryi, H.; Kaplan, N. A.; Podleschny, M.; Liu, X.; Wehner, P.; Borchers, A.; Tolwinski, N. S. PTK7/Otk Interacts with Wnts and Inhibits Canonical Wnt Signalling. *EMBO J* **2011**, *30* (18), 3729–3740. https://doi.org/10.1038/emboj.2011.236.

(23) Hayes, M.; Naito, M.; Daulat, A.; Angers, S.; Ciruna, B. Ptk7 Promotes Non-Canonical Wnt/PCP-Mediated Morphogenesis and Inhibits Wnt/β-Catenin-Dependent Cell Fate Decisions during Vertebrate Development. *Development* **2013**, *140* (8), 1807–1818. https://doi.org/10.1242/dev.090183.

(24) Bin-Nun, N.; Lichtig, H.; Malyarova, A.; Levy, M.; Elias, S.; Frank, D. PTK7 Modulates Wnt Signaling Activity via LRP6. *Development* **2014**, *141* (2), 410–421. https://doi.org/10.1242/dev.095984.

(25) Machleidt, T.; Woodroofe, C. C.; Schwinn, M. K.; Méndez, J.; Robers, M. B.; Zimmerman, K.; Otto, P.; Daniels, D. L.; Kirkland, T. A.; Wood, K. V. NanoBRET--A Novel BRET Platform for the Analysis of Protein-Protein Interactions. *ACS Chem Biol* **2015**, *10* (8), 1797–1804. https://doi.org/10.1021/acschembio.5b00143.

(26) El Turk, F.; Fauvet, B.; Ouertatani-Sakouhi, H.; Lugari, A.; Betzi, S.; Roche, P.; Morelli, X.; Lashuel, H. A. An Integrative in Silico Methodology for the Identification of Modulators of Macrophage Migration Inhibitory Factor (MIF) Tautomerase Activity. *Bioorg Med Chem* **2010**, *18* (14), 5425–5440. https://doi.org/10.1016/j.bmc.2010.05.010.

(27) Bosc, N.; Muller, C.; Hoffer, L.; Lagorce, D.; Bourg, S.; Derviaux, C.; Gourdel, M.-E.; Rain, J.-C.; Miller, T. W.; Villoutreix, B. O.; Miteva, M. A.; Bonnet, P.; Morelli, X.; Sperandio, O.; Roche, P. Fr-PPIChem: An Academic Compound Library Dedicated to Protein-Protein Interactions. *ACS Chem Biol* **2020**, *15* (6), 1566–1574. https://doi.org/10.1021/acschembio.0c00179.

(28) Yan, M.; Li, G.; An, J. Discovery of Small Molecule Inhibitors of the Wnt/β-Catenin Signaling Pathway by Targeting β-Catenin/Tcf4 Interactions. *Exp. Biol. Med. (Maywood)* **2017**, *242* (11), 1185–1197. https://doi.org/10.1177/1535370217708198.

(29) Pfleger, K. D. G.; Eidne, K. A. Illuminating Insights into Protein-Protein Interactions Using Bioluminescence Resonance Energy Transfer (BRET). *Nat Methods* **2006**, *3* (3), 165–174. https://doi.org/10.1038/nmeth841.

(30) Korb, O.; Stützle, T.; Exner, T. E. Empirical Scoring Functions for Advanced Protein-Ligand Docking with PLANTS. *J Chem Inf Model* **2009**, *49* (1), 84–96. https://doi.org/10.1021/ci800298z.

(31) Wolber, G.; Langer, T. LigandScout: 3-D Pharmacophores Derived from Protein-Bound Ligands and Their Use as Virtual Screening Filters. *J Chem Inf Model* **2005**, *45* (1), 160–169. https://doi.org/10.1021/ci049885e.

(32) Morin, P. J.; Sparks, A. B.; Korinek, V.; Barker, N.; Clevers, H.; Vogelstein, B.; Kinzler, K. W. Activation of Beta-Catenin-Tcf Signaling in Colon Cancer by Mutations in Beta-Catenin or APC. *Science* **1997**, *275* (5307), 1787–1790. https://doi.org/10.1126/science.275.5307.1787.

(33) Smith, K. J.; Johnson, K. A.; Bryan, T. M.; Hill, D. E.; Markowitz, S.; Willson, J. K.; Paraskeva, C.; Petersen, G. M.; Hamilton, S. R.; Vogelstein, B. The APC Gene Product in Normal and Tumor Cells. *Proc Natl Acad Sci U S A* **1993**, *90* (7), 2846–2850. https://doi.org/10.1073/pnas.90.7.2846.

(34) Thorne, C. A.; Hanson, A. J.; Schneider, J.; Tahinci, E.; Orton, D.; Cselenyi, C. S.; Jernigan, K. K.; Meyers, K. C.; Hang, B. I.; Waterson, A. G.; Kim, K.; Melancon, B.; Ghidu, V. P.; Sulikowski, G. A.; LaFleur, B.; Salic, A.; Lee, L. A.; Miller, D. M.; Lee, E. Small-Molecule Inhibition of Wnt Signaling through Activation of Casein Kinase 1α. *Nat Chem Biol* **2010**, *6* (11), 829–836. https://doi.org/10.1038/nchembio.453.

(35) Jho, E.; Zhang, T.; Domon, C.; Joo, C.-K.; Freund, J.-N.; Costantini, F. Wnt/Beta-Catenin/Tcf Signaling Induces the Transcription of Axin2, a Negative Regulator of the Signaling Pathway. *Mol Cell Biol* **2002**, *22* (4), 1172–1183. https://doi.org/10.1128/MCB.22.4.1172-1183.2002.

(36) Moreau, M.; Mourah, S.; Dosquet, C. β-Catenin and NF-KB Cooperate to Regulate the UPA/UPAR System in Cancer Cells. *Int J Cancer* **2011**, *128* (6), 1280–1292. https://doi.org/10.1002/ijc.25455.

(37) Vivekanandhan, S.; Yang, L.; Cao, Y.; Wang, E.; Dutta, S. K.; Sharma, A. K.; Mukhopadhyay, D. Genetic Status of KRAS Modulates the Role of Neuropilin-1 in Tumorigenesis. *Sci Rep* **2017**, *7* (1), 12877. https://doi.org/10.1038/s41598-017-12992-2.

(38) Sikandar, S.; Dizon, D.; Shen, X.; Li, Z.; Besterman, J.; Lipkin, S. M. The Class I HDAC Inhibitor MGCD0103 Induces Cell Cycle Arrest and Apoptosis in Colon Cancer Initiating Cells by Upregulating Dickkopf-1 and Non-Canonical Wnt Signaling. *Oncotarget* **2010**, *1* (7), 596–605. https://doi.org/10.18632/oncotarget.101001.

(39) Davidson, G.; Niehrs, C. Emerging Links between CDK Cell Cycle Regulators and Wnt Signaling. *Trends Cell Biol* **2010**, *20* (8), 453–460. https://doi.org/10.1016/j.tcb.2010.05.002.

(40) Orford, K.; Orford, C. C.; Byers, S. W. Exogenous Expression of Beta-Catenin Regulates Contact Inhibition, Anchorage-Independent Growth, Anoikis, and Radiation-Induced Cell Cycle Arrest. *J Cell Biol* **1999**, *146* (4), 855–868. https://doi.org/10.1083/jcb.146.4.855.

(41) Shiheido, H.; Takashima, H.; Doi, N.; Yanagawa, H. MRNA Display Selection of an Optimized MDM2-Binding Peptide That Potently Inhibits MDM2-P53 Interaction. *PLoS One* **2011**, *6* (3), e17898. https://doi.org/10.1371/journal.pone.0017898.

(42) Takimoto, R.; Wang, W.; Dicker, D. T.; Rastinejad, F.; Lyssikatos, J.; el-Deiry, W. S. The Mutant P53-Conformation Modifying Drug, CP-31398, Can Induce Apoptosis of Human Cancer Cells and Can Stabilize Wild-Type P53 Protein. *Cancer Biol Ther* **2002**, *1* (1), 47–55. https://doi.org/10.4161/cbt.1.1.41.

(43) Kim, W. K.; Byun, W. S.; Chung, H.-J.; Oh, J.; Park, H. J.; Choi, J. S.; Lee, S. K. Esculetin Suppresses Tumor Growth and Metastasis by Targeting Axin2/E-Cadherin Axis in Colorectal Cancer. *Biochem Pharmacol* **2018**, *152*, 71–83. https://doi.org/10.1016/j.bcp.2018.03.009.

(44) Faber, A. C.; Coffee, E. M.; Costa, C.; Dastur, A.; Ebi, H.; Hata, A. N.; Yeo, A. T.; Edelman, E. J.; Song, Y.;

Tam, A. T.; Boisvert, J. L.; Milano, R. J.; Roper, J.; Kodack, D. P.; Jain, R. K.; Corcoran, R. B.; Rivera, M. N.; Ramaswamy, S.; Hung, K. E.; Benes, C. H.; Engelman, J. A. MTOR Inhibition Specifically Sensitizes Colorectal Cancers with KRAS or BRAF Mutations to BCL-2/BCL-XL Inhibition by Suppressing MCL-1. *Cancer Discov* **2014**, *4* (1), 42–52. https://doi.org/10.1158/2159-8290.CD-13-0315.

(45) Hata, A. N.; Engelman, J. A.; Faber, A. C. The BCL2 Family: Key Mediators of the Apoptotic Response to Targeted Anticancer Therapeutics. *Cancer Discov* **2015**, *5* (5), 475–487. https://doi.org/10.1158/2159-8290.CD-15-0011.

Insert Table of Contents artwork here

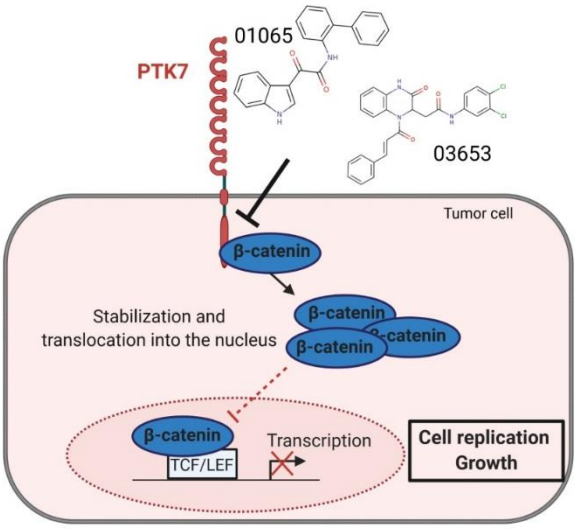

Discovery of small molecule inhibitors of the PTK7/β-catenin interaction targeting the Wnt signaling pathway in colorectal cancer

Laetitia Ganier[1,2], Stéphane Betzi[2,3], Carine Derviaux[3], Philippe Roche[2,3], Charlotte Dessaux[1], Christophe Muller[3,†], Laurent Hoffer[2,‡], Xavier Morelli[2,3],* and Jean-Paul Borg[1,4] *

[1]Aix Marseille Univ, CNRS, INSERM, Institut Paoli-Calmettes, CRCM, Equipe labellisée Ligue 'Cell polarity, Cell signaling and Cancer', Marseille, France

[2]Aix Marseille Univ, CNRS, INSERM, Institut Paoli-Calmettes, CRCM, team 'Integrative Structural and Chemical Biology', Marseille, France

[3]Aix Marseille Univ, CNRS, INSERM, Institut Paoli-Calmettes, CRCM, 'HiTS/IPCdd – High throughput screening platform', Marseille, France

[4] Institut Universitaire de France

**Corresponding authors: jean-paul.borg@inserm.fr and xavier.morelli@inserm.fr

Supporting Information

Table of contents

I. MATERIALS AND METHODS

Cell lines and reagents

HEK293T and SW480 were cultured in DMEM supplemented with 10%FBS. HCT116 were cultured in RPMI supplemented with 10% FBS. Mouse embryo fibroblasts (MEFs) were cultured in DMEM supplemented with 15% FBS, 1% sodium pyruvate, 1% non-essential amino acids and 50µM 2-mercaptoethanol. All cells were grown at 37°C under 5% CO_2 with relative humidity.

The Fr-PPIChem library resulted from a French consortium including present authors to create a unique chemical library dedicated to the inhibition of protein-protein interactions (PPIs)[1]. The Fr-PPIChem library is available upon request in 384-well plates. Pyrvinium was purchased from Sigma-Aldrich.

The siRNA sequence for PTK7 used was no. 25 : 5'-ACGUGGUAGUAGCGAGGUA-3' (Horizon Discovery Ltd).

In silico structure-based screening

The *in-silico* screening was designed based on a strategy described previously and combines three robust computational approaches : molecular dynamics (MD) simulations, molecular docking and pharmacophore filtering [2]. We performed MD simulations of PTK7 in periodic conditions in explicit aqueous solvent using the CHARMM force field starting from the X-ray structure of unliganded, inactive PTK7 kinase domain (pdb code : 6VG3)[3]. The initial structure was prepared with MOE software (https://www.chemcomp.com/). The protein was solvated in a TIP3P water box containing chloride and sodium ions to ensure a neutral system. This step and inputs for MD production stage were prepared with the Charmm-gui server (https://www.charmm-gui.org/). Electrostatic interactions were treated using the particle-mesh Ewald summation method, and we used the switch function for the van der Waals energy interactions with cuton, cutoff and cutnb values of 10, 12 and 14 Å, respectively. The Shake algorithm was applied to all hydrogen-containing bonds. The system was equilibrated at 330K for 2 ns followed by a production phase of 50ns using 2 fs integration step. Coordinates were saved every 0.5 ps for subsequent analysis.

We performed a clustering analysis of the MD ensemble to reduce the number of conformations to be used as receptors in high-throughput docking. The clustering analysis was mainly aimed at separating the 'open' from 'closed' conformations and thus revealing cryptic pockets. KMeans was used as the clustering method and a threshold similarity of 1.5Å was chosen. Analysis of

cavities presence and frequency of opening among all frames with F-pocket[4] and MDpocket[5] led to the identification of two druggable pockets more accessible based on the RMSD. The high-throughput molecular docking step was performed on the surface of the previously 10 minimized and optimal PTK7 protein structures using PLANTS[6] and MOE (https://www.chemcomp.com/) on the 10,314 compounds from the Fr-PPIChem library. A maximum of 10 poses were generated by the docking algorithm for each compound followed by selection of the top ranked pose for each compound. PLANTS initial scoring and MOE rescoring led to a consensus and selection of the 200 best ligands. Each generated model was then subjected to a structure-based pharmacophore filtering using LigandScout[7]. Criteria for compound selection were more than 2 interactions or original interaction within the protein cavity leading to a final set of 100 compounds of which 92 were available in the MolPort database (https://www.molport.com/). These compounds were purchased and tested experimentally by NanoBRET™.

NanoBRET™ assay

The initial development of the NanoBRET™ assay to detect the interaction of PTK7 and β-catenin in transiently-transfected HEK293 cells was done with Promega. The NanoBRET™ protocol was adapted from a technical manual optimized by Promega for the detection of PTK7/βcatenin interaction.

HEK293T cells were resuspend to a final density of $4x10^5$ cells/mL in cell culture medium and 2mL (800,000 cells) were plated into a well of a six-well plate. Cells were allowed to attach and recover for 4-6 hours at 37°C, 5% CO_2 and humidity. Cells were transfected using Lipofectamine® LTX & PLUS™ reagent (ThermoFischer Scientific). A first transfection mixture containing 300µL of Opti-MEM® Reduced Serum Medium (no phenol red) with 2µg of PTK7 acceptor vector, 0,2µg of β-catenin donor vector and 3µL of PLUS™ reagent and a second one containing 300µL of Opti-MEM® Reduced Serum Medium phenol-free with 6µL of Lipofectamine® LTX reagent were prepared. The mixtures are mixed and incubated at room temperature for 10 minutes. The transfection mixture is added to wells with attached cells and proteins are expressed for approximately 20-24hours at 37°C, 5% CO_2 and humidity. For larger scale experiments, cells were transfected in $10cm^2$ dishes with adapted quantity of cells and transfection reagents accordingly.

The next day, cells were trypsinized, washed in complete media, and re-suspended in OptiMEM phenol-free containing 4% FBS at a density of $2x10^5$ cells/mL. HaloTag 618 ligand was then added to the cell suspension (1µL/mL of 0.1mM stock solution), and 39,5µL of the cell mixture was plated per well of a 384-well white-walled tissue culture plate. For the "no-acceptor controls",

1µL of DMSO were added per mL of cells. When needed, compounds are added in 384-well white-walled tissue culture plate beforehand at the desired concentration with the Labcyte Echo® Acoustic Liquid Handling and adjusted to a final concentration of 1%DMSO (maximum tolerated). For vehicle control, 1% DMSO was added to the cells. Plates were then incubated overnight for maximum compound effect. To measure BRET signal, the Nano-Glo substrate was diluted in OptiMEM phenol-free (10µL/mL) and 10µL of the mixture was added to each well. Donor (460nm) and acceptor (618nm) emissions were measured using the PHERAstar® FSX microplate reader (BMG LABTECH). To calculate raw NanoBRET™ ratio values, the acceptor emission value is divided by the donor emission value for each sample.

The Z-factor is defined as: Z-factor = $1 - [3(\sigma_p + \sigma_n)/(\mu_p - \mu_n)]$.

TopFlash assay

Canonical Wnt/β-catenin signaling activation was evaluated using transient transfection of reporter plasmids. HCT116 (1×10^5 cells/well) and SW480 (7×10^4 cells/well) were seeded in 24-well plates and transfected with siPTK7 #25 using Lipofectamine® RNAi max (ThermoFischer Scientific) when needed. After 48h, cells were transfected with 500ng of TK-luciferase (firefly) reporter plasmid containing wild-type (TOPflash) TCF/LEF binding sites or containing mutated TCF/LEF binding sites (FOPFlash) and 70ng of Renilla luciferase reporter plasmid (as transfection efficiency reporter) using Lipofectamine® LTX and plus reagent (ThermoFischer Scientific). These plasmids were a nice gift from Christophe Ginestier. 8h later transfection medium was replaced wish fresh medium containing the different drugs and positive controls at indicated concentrations or 1% DMSO for incubation overnight. Renilla and Firefly luciferase expression were revealed using Dual-Luciferase Reporter assay (Promega) according to the manufacturer's instructions and measured using a CLARIOstar microplate reader (BMG LABTECH). Data are expressed as (TOPflash Luciferase Firefly/Renilla ratio) / (FOPflash Luciferase Firefly/Renilla ratio) ratio normalized to DMSO treated cells.

Cell viability assay

HCT116 (7×10^3 cells/well), SW480 (5×10^3 cells/well) and MEFs (1×10^4 cells/well) were seeded in 96-well plates (Corning®) and incubated for 24h. Cells were treated with a range of concentrations of drugs with a dilution factor of 2 (1,87-60 µM). After 72 hours drug incubation, metabolic activity was detected by addition of 25µL/well of Alamar Blue and fluorescence intensity was measured using a CLARIOstar microplate reader (BMG LABTECH). Cell viability was determined and expressed as a percentage of control cells treated with 1% DMSO.

Colony formation assay in soft agar

HCT116 and SW480 cells were seeded in 6-well plates (Corning®) and incubated for 48 hours. Cells were treated overnight with DMSO or the candidate inhibitors. 96-well plates white with transparent bottom were covered with a layer of 0,6% agarose. HCT116 and SW480 cells were seeded at 500 and 1000 cells/well, respectively, into a layer of 0,36% agarose. A feeder layer at the same concentration of agarose was supplemented above the cells. After culturing HCT116 and SW480 cells for 6 and 15 days, respectively, colonies consisting of more than 50 cells were visualized using a microscope (Olympus CX-41, PLCN4X objective) and quantified with CellTiter-Glo® 3D Cell Viability Assay (Promega).

RT-qPCR

HCT116 and SW480 cells were seeded in 6-well plates (Corning®) and incubated for 24h. Cells were treated with candidate inhibitors or DMSO for 24h. Total RNA was isolated using the RNeasy mini kit (Qiagen) according to the manufacturer's instructions and treated with DNase1. Total RNA was quantified on NanoDROP spectrophotometer ND-1000 (Thermo Fischer Scientific). After heat activation, total RNA was reverse transcribed to the first-strand cDNA using SuperScript™ II First-Strand Synthesis system (Thermo Fischer Scientific) with random primers (Thermo Fischer Scientific). The reverse transcribed product is used to run real time PCR reactions using SYBR Green mastermix (ThermoFischer Scientific) on a Biorad CFX96™ real-time cycler. Primers obtained from Life Technologies/ThermoFischer Scientific are listed in **Table S4**.

RT² Profiler PCR arrays

Preparation of samples and RNA extraction are done similarly than in RT-qPCR section. Single-stranded cDNA is synthesized from all samples using the RT² First Strand Kit (Qiagen) as described in the Qiagen protocol for RT² profiler array sample preparation. The reverse transcribed product is used to run real time PCR reactions using RT² SYBR Green qPCR mastermix (Qiagen) on a Biorad CFX96™ real-time cyclers.

Flow cytometry analysis

HCT116 and SW480 cells were seeded in 6-well plates (Corning®) and incubated for 24h. For analysis of the cell cycle, cells were treated with candidate inhibitors or DMSO for 24h. After treatment, cells were trypsinized and permeabilize with the eBioscience™ Foxp3 / Transcription

Factor Fixation / Permeabilization kit (ThermoFisher Scientific). Briefly, cells were incubated for 20min at 4°C in 1mL of permeabilization buffer. Then, cells were washed in 2mL of Wash buffer 1X diluted in PBS-1% BSA. Cells were stained for 20min at RT in 200µL of wash buffer 1X containing 40µg/mL of propidium iodide and 40µg/mL of RNase A (DNase and protease-free) (ThermoFisher Scientific) and analyzed on a BD™ LSRII flow cytometer.

For apoptosis analysis, cells were treated with candidate inhibitors or DMSO for 48h. Cells were stained for 15min at RT in 100µL of Annexin-binding buffer containing 1µg/mL of propidium iodide and 5µL/assay of Annexin V FITC and analyzed on a BD™ LSRII flow cytometer.

Immunoblot analysis

Cells were lysed in ice-cold lysis buffer containing 50mM Tris pH7.5, 0,5M NaCl, 1% Igepal, 1% Deoxycholic acid, 0,1% SDS, 2mM EDTA, Proteinase and Phosphatase Inhibitor Cocktail. Typically, 25µg cell lysates were migrated in SDS-PAGE (Sodium Dodecyl Sulfate-PolyAcrylamide Gel Electrophoresis), with variable % depending on the proteins analyzed, and transferred onto Amersham™ Protran™ Supported 0.45 µM or 0.2µM NC (GE Healthcare BioSciences). The primary antibodies used are listed in **Table S5**.

Statistical analysis

All graphs and statistical analyses were done using the GraphPad Prism™ software. All data are presented as mean of multiple experiments (+/- standard deviation). Statistical tests used for determination of P-values are specified in corresponding figure legends. For all analyses, only P-values <0.05 were considered as statistically significant, the key for asterisk placeholders for P-values in the figures are: ***P<0.001, ** P<0.01, * P<0.05.

II. SUPPLEMENTARY FIGURES

Figure S1 (Ganier *et al.*)

A

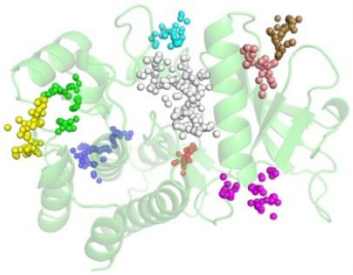

Pocket	Druggability score
Pocket 1	0.749
Pocket 2	0.210
Pocket 3	0.016
Pocket 4	0.493
Pocket 5	0.087
Pocket 6	0.276
Pocket 7	0.057
Pocket 8	0.049
Pocket 9	0.017

B

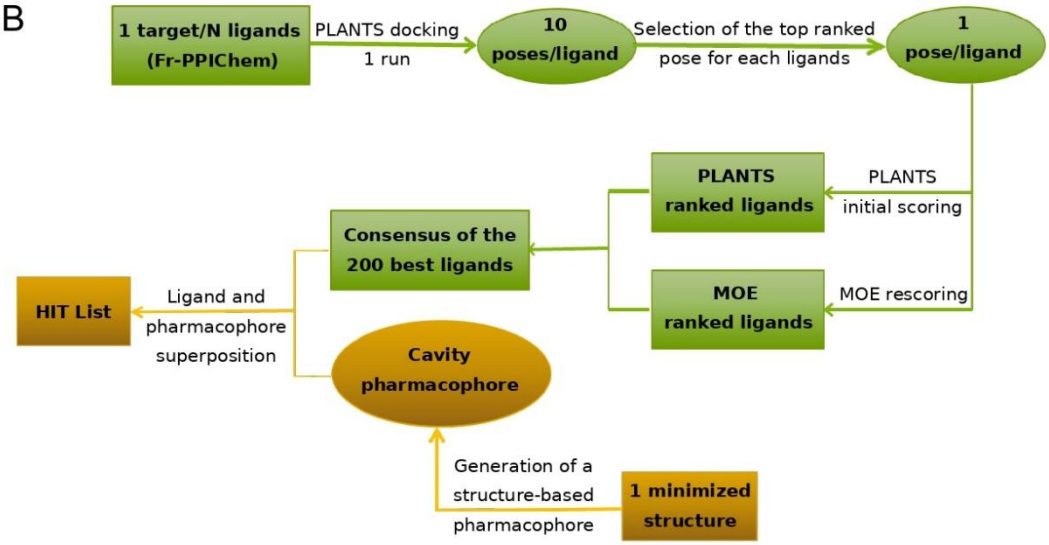

Figure S1. (A-B) ***In silico* screening workflow** (A) The first step consisted in MD simulations of PTK7 to account for the structural flexibility of the protein and reveal potential cryptic pockets. Pockets detected in the MD conformations starting from the X-ray structure of unliganded inactive PTK7 kinase domain with FPocket/MDPocket are shown together with the associated druggability score. Pockets 1 and 2 were selected for subsequent docking studies based on the accessibility of these pockets to small molecules. (B) The second step consisted in high-throughput molecular docking of the Fr-PPIChem library[1]. This step was performed on the surface of optimal PTK7 protein structures identified previously using PLANTS[6] and MOE (https://www.chemcomp.com) to generate several compounds conformations that would fit each compound of the chemical library into the two binding pockets identified. This led to a consensus and selection of the 200 best ligands. Finally, the last step subjected each generated model to our structure-based pharmacophore filtering using LigandScout[7] which led to our final hit list.

Figure S2 (Ganier *et al.*)

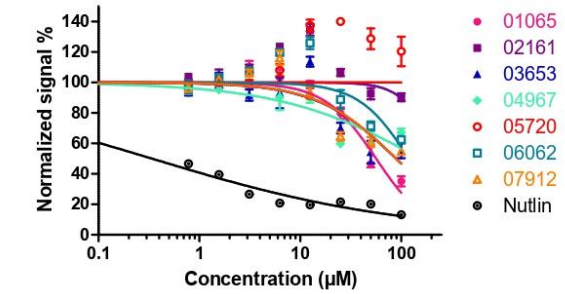

Figure S2. Evaluation of hit compounds selectivity (A) BRET signal in transiently transfected HEK293 cells with p53-HT and NL-MDM2 plasmids incubated overnight with increasing concentrations of compounds. Values are mean ± SD, n=3.

Figure S3 (Ganier *et al.*)

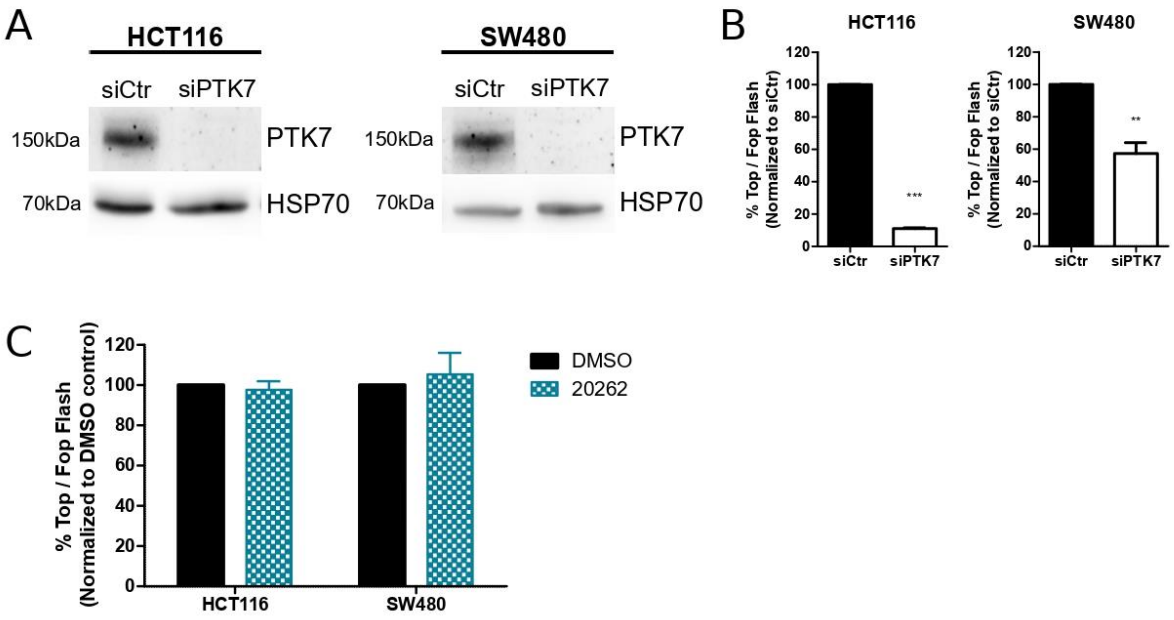

Figure S3. Identification of PTK7/β-catenin inhibitors targeting Wnt pathway signaling in CRC cells (A) PTK7 siRNA KD efficiency was evaluated by western blot analysis. HSP70 was used as a loading control. (B) WNT signaling measured by TopFlash assay normalized with FOP activity on HCT116 and SW480 cells treated for 48h with siPTK7 or siCtr. (C) HCT116 and SW480 were incubated overnight with the compound 20262 at 25µM. WNT signaling activity was measured as reported in Figure 2C.

Figure S4 (Ganier *et al.*)

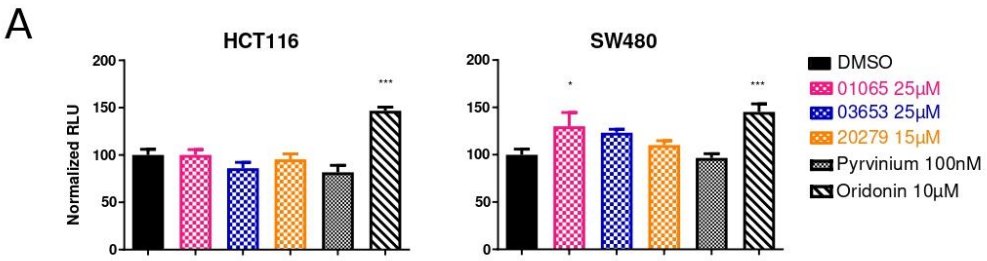

Figure S4. PTK7/β-catenin inhibitors impair anchorage-independent cell growth and proliferation. (A) HCT116 and SW480 cells were quantified with CellTiter-Glo® 3D Cell Viability Assay (Promega) at Day 0 of the soft agar colony formation assay to exclude a potential effect of compounds cytotoxicity. Bar graphs indicate luciferase activities expressed in relative light units (RLUs), relative to activities measured in DMSO control after treatment overnight with DMSO, 25µM of 01065 and 03653, 15µM of 20279, 100nM of pyrvinium or 10µM of Oridonin. Results are expressed as mean of 2 independent experiments ± SD and *P* values are derived from one-way Anova (*p <0.05; ***p < 0.001).

Figure S5 (Ganier *et al.*)

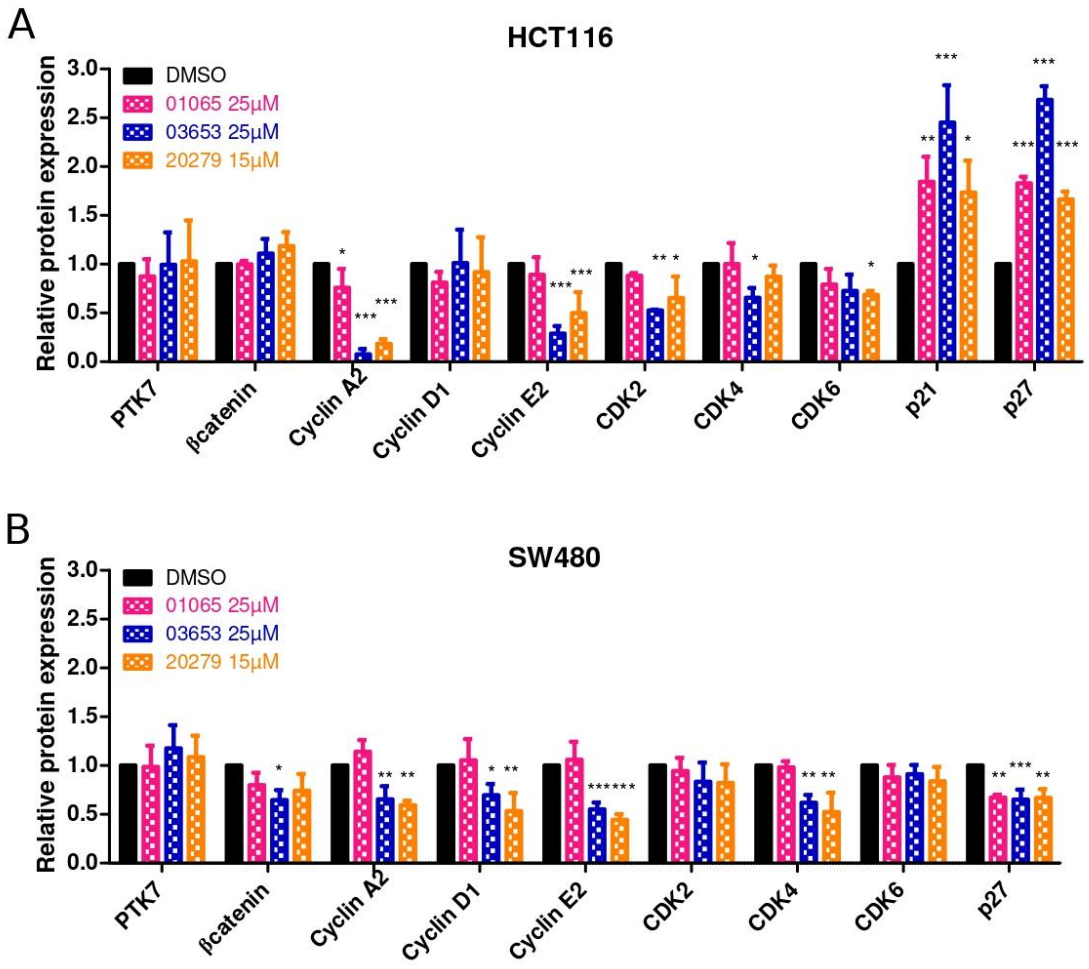

Figure S4. PTK7/β-catenin inhibitors cause cell cycle arrest in CRC cells. (A-B) Quantifications of western blot analysis in HCT116 (A) and SW480 (B) were performed using Image J software and are represented as histograms of relative protein expression normalized to DMSO control. Results are expressed as mean of 3 independent experiments ± SD and *P* values are derived from one-way Anova (*p < 0.05; **p <0.01; ***p < 0.001).

Figure S6 (Ganier *et al.*)

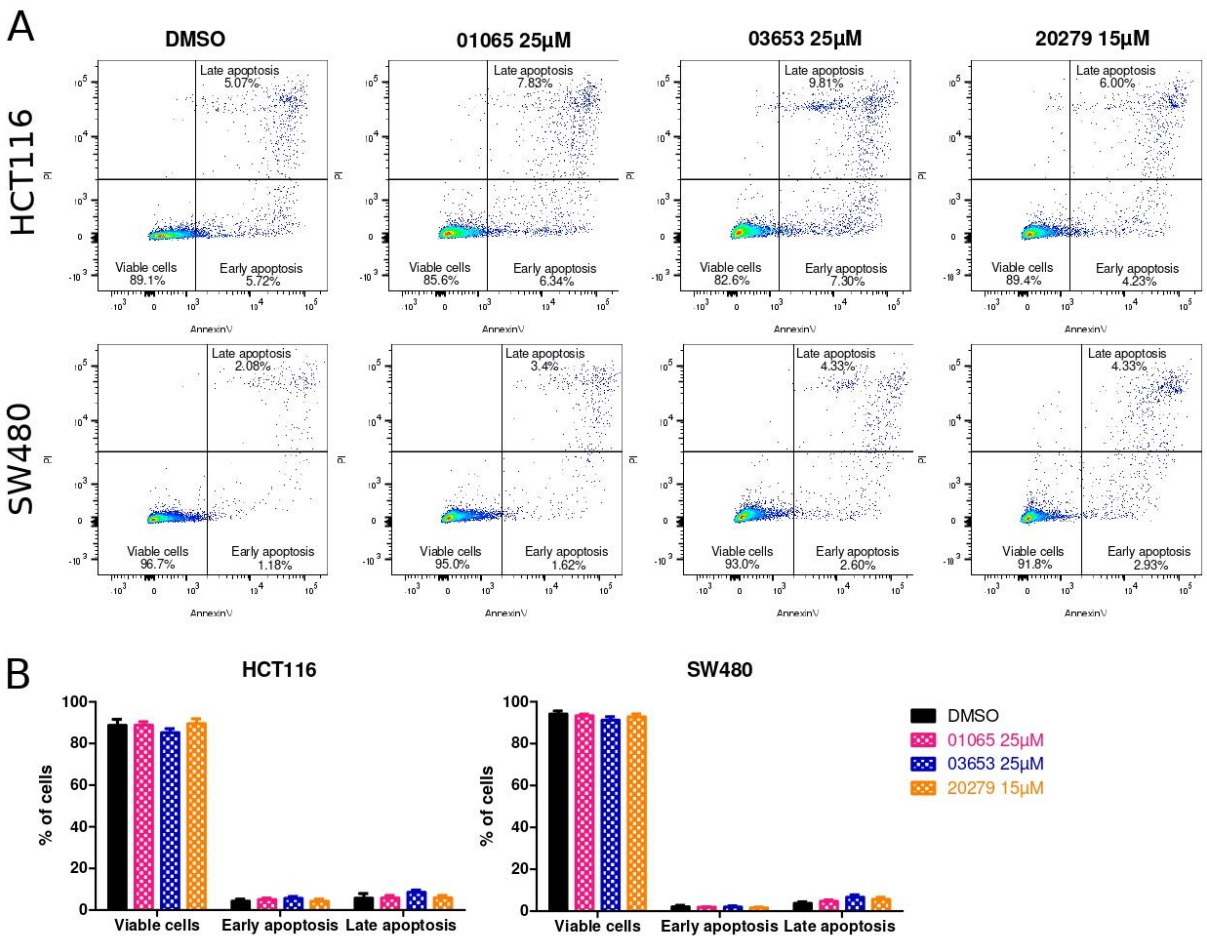

Figure S5. PTK7/β-catenin inhibitors do not induce cell apoptosis following cell cycle arrest. (A-B) Effect of compounds 01065, 03653 and 20279 on apoptosis of HCT116 and SW480 cells. Cells were treated for 48h with the different compounds and stained with Annexin V-FITC and propidium iodide before being quantified by flow cytometry. (A) Dot plots were divided into four quadrants to indicate viable cells, early apoptosis and late apoptosis. (B) Cell viability distribution is represented as histogram of the percentage of viable, early apoptotic and late apoptotic cells. Results are expressed as mean of 3 independent experiments ± SEM and are not statistically different between the DMSO and treated groups.

III. Supplementary Tables

Table S1: Small molecule inhibitors targeting β-catenin/TCF4 interaction tested in NanoBRET™ for their cross-reactivity on the PTK7/β-catenin interaction.

Compound name	Structure	Specificity	IC50 (µM) NanoBRET PTK7/β-catenin	References
PKF118-310 (Toxoflavin)	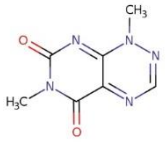	TCF4	101.5	8
LF3	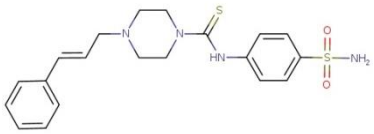	TCF4 Lef1	111.7	9
iCRT3	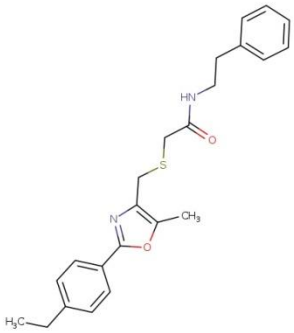	TCF4 Ecadherin +/- αcatenin +/-	64.19	10
iCRT14	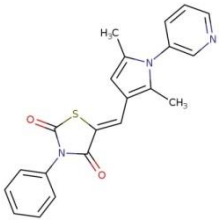	TCF4 Ecadherin +/- αcatenin +/-	101.1	10
R999636	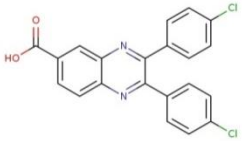	TCF4 E-cadherin APC +/-	89.48	11
L338192	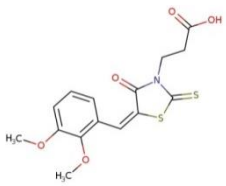	TCF4 APC E-cadherin +/-	N/D	11

PNU-47654	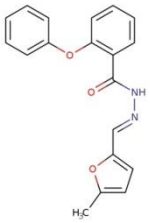	No data	N/D	12

Table S2: Selection of compounds from *Vitas-M Laboratory, Ltd.* to probe the structure-activity relationship (SAR)

Compound name	Hits	Structure	Molecular Weight	IC50 (µM) NanoBRET
20238	01065	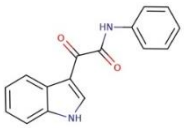	264.28	177.1
20269	01065	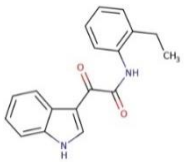	292.34	**19.39***
20270	01065	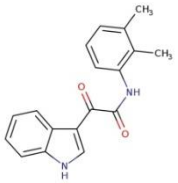	292.34	N/D
20271	01065	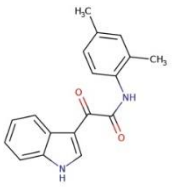	292.34	N/D
20272	01065		292.34	N/D
20273	01065	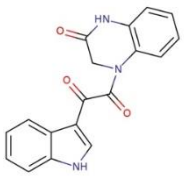	319.32	$2.6X10^{9}$
20274	01065	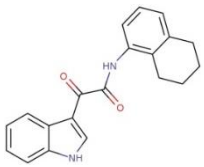	318.38	**12.66***
20285	1065	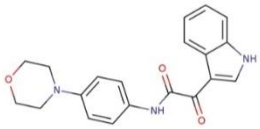	349.39	N/D

20240	02161	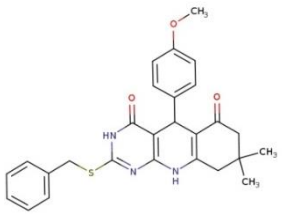	473.59	$1x10^5$
20241	02161	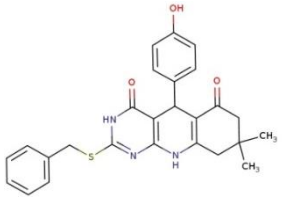	459.56	142.3
20242	02161	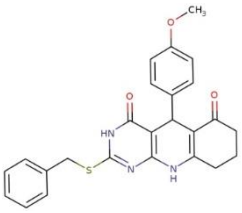	445.54	94.02
20243	02161	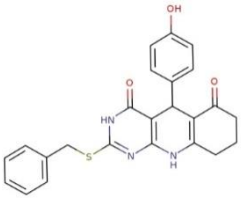	431.51	$3.5x10^4$
20244	02161	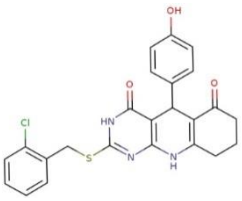	465.95	174.2
20245	02161	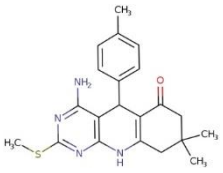	380.51	155.1
20246	02161	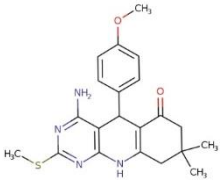	396.51	N/D
20247	02161	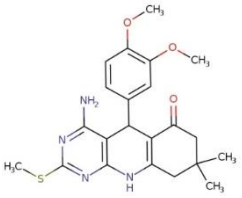	426.54	N/D

20248	02161	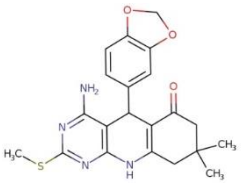	410.49	117.6
20249	02161	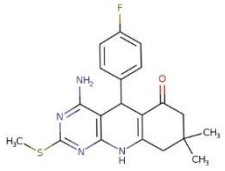	384.47	137.5
20250	02161	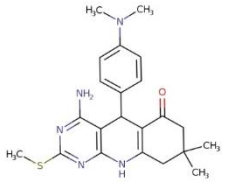	409.55	252.6
20251	02161		396.51	$1.5x10^4$
20252	02161	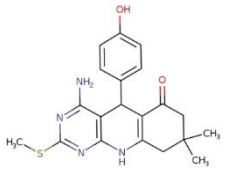	382.48	N/D
20254	03653	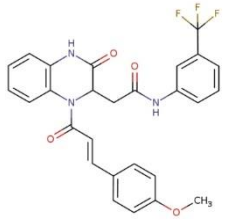	509.48	86.89
20255	03653	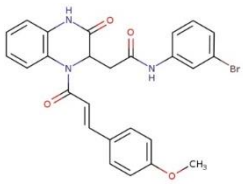	520.38	N/D
20256	03653	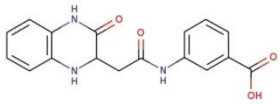	325.32	N/D
20257	03653	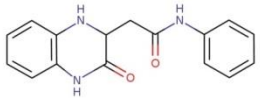	281.32	N/D

20262	03653	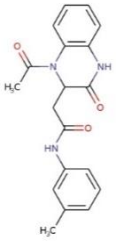	337.38	N/D
20263	03653	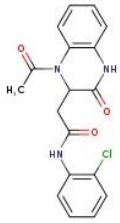	357.79	107.7
20275	03653	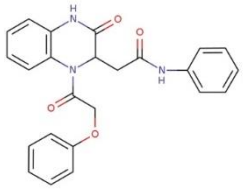	415.45	$9x10^5$
20277	03653	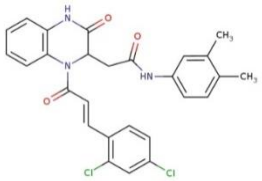	508.4	49.38
20278	03653	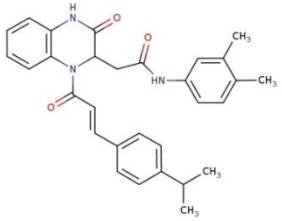	481.6	**37.88***
20279	03653	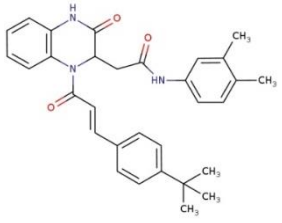	495.62	**17.28***
20280	03653	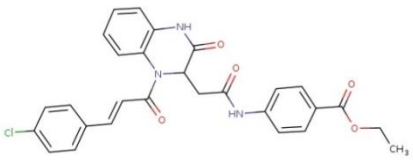	517.97	97.42
20239	04967	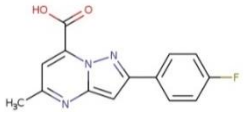	271.25	2204

20266	04967	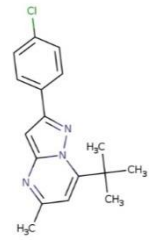	299.8	$1x10^7$
20276	04967	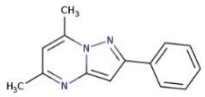	223.28	$1x10^4$
20281	04967	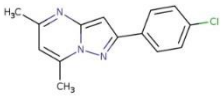	257.72	$1.2x10^5$
20284	04967	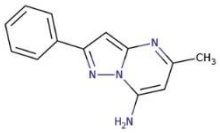	224.27	$4.5x10^5$
20260	05720	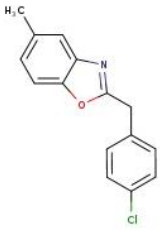	257.72	344.9
20268	05720	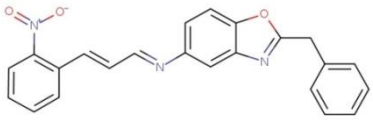	383.41	57.31
20282	05720	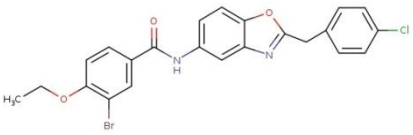	485.76	51.13
20283	05720	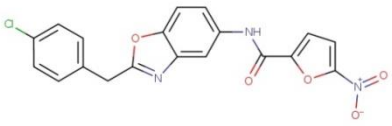	397.77	29.3
20286	05720	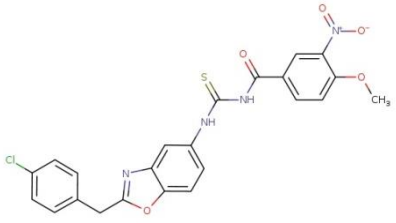	496.92	105.7

20287	05720	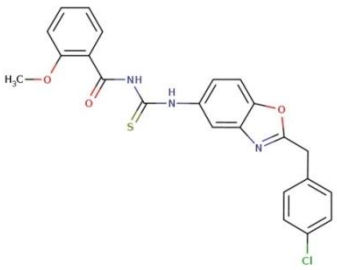	451.93	N/D
20258	06062	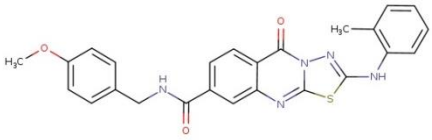	471.54	55.52
20259	06062	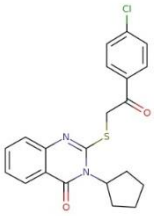	398.91	$6.4x10^{24}$
20261	06062	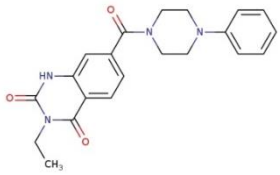	378.43	N/D
20264	06062	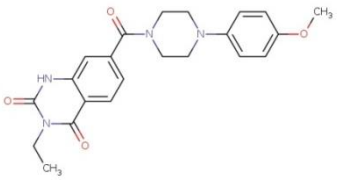	408.46	125
20265	06062	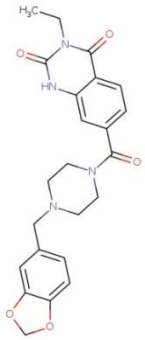	436.47	86.98
20267	06062	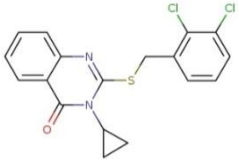	377.28	129.3

20288	07912	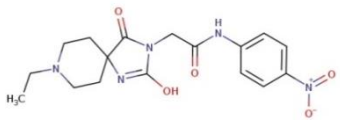	375.38	N/D
20289	07912	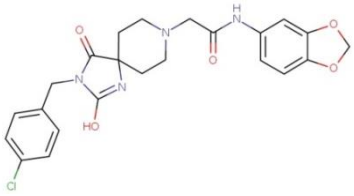	470.91	78.62
20290	07912	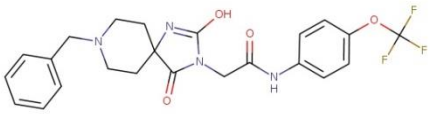	476.46	77.3
20291	07912	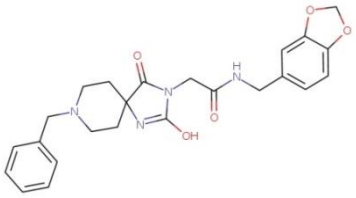	450.5	757.5
20292	07912	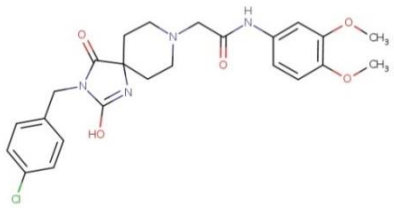	486.95	175.1
20293	07912	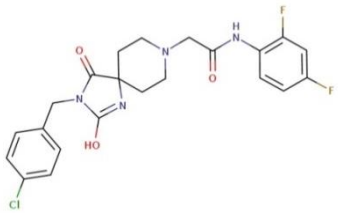	462.88	75.24

Table S3: List of the 84 key genes responsive to WNT signal transduction in the RT² Profiler PCR Array and associated functions

Cell Adhesion Molecules	ABCB1, CD44, CDH1, CCN2, NRCAM
Cell Migration	CD44, EFNB1, EGFR, FN1, IRS1, NRCAM, NRP1, PDGFRA, VEGFA
Cell Cycle	AHR, BIRC5, CCND1, CCND2, EGFR, FOSL1, ID2, MYC, PTGS2
Differentiation & Development	Growth Factors : ANGPTL4, BMP4, CCN2, FGF20, FGF4, FGF7, FGF9, GDF5, GDNF, IGF1, IGF2, IL6, JAG1, TGFB3, VEGFA Transcription Factors : CDKN2A, EGR1, NANOG, POU5F1, RUNX2, SIX1, SOX2, SOX9, TBXT, TWIST1 Others : ANTXR1, CDON, DAB2, DLK1, EFNB1, FN1, GJA1, ID2, MET, NTRK2, PDGFRA
Calcium Binding & Signaling	BGLAP, CACNA2D3, CUBN, EGFR
Proteases	DPP10, MMP3, MMP7, MMP9, PLAUR
Signal Transduction	WNT signaling : AXIN2, BTRC, CCN4, CCN5, DKK1, FZD7, LRP1, PLPP3, SFRP2, TLE1, WNT3A, WNT5A, WNT9A TGFβ Signaling : BMP4, FST, GDF5, GDNF, TGFB3 Hedgehog Signaling : PTCH1, SMO Notch Signaling : JAG1
Transcription Factors	WNT Signaling : LEF1, TCF7, TCF7L1, TCF7L2 Others : CEBPD, ETS2, KLF5, MYC, PITX2, PPARD, TCF4

Table S4: Primer sequences

Gene		Sequence
PTK7		For 5'-CAGTTCCTGAGGATTTCCAAGAG-3' Rev 5'-TGCATAGGGCCACCTTC-3'
CTNNB1		For 5’-ATTGGCAATGAGCGGTTCCG-3’ Rev 5’-AGGGCAGTGATCTCCTTCTG-3’
AXIN2		For 5'-AGTGTGAGGTCCACGGAAAC-3' Rev 5'-CTTCACACTGCGATGCATTT-3'
PLAUR		For 5'-CTGCAAGGGGAACAGCAC-3' Rev 5'-GCTTTGGTTTTTCGGTTCG-3'
FOSL1		For 5'-CTTGTGAACAGATCAGCCCG-3' Rev 5'-TCCAGTTTGTCAGTCTCCGC-3'
DKK1		For 5’-CAACGCTATCAAGAACCTGC-3’ Rev 5’-GATCTTGGACCAGAAGTGTC-3’
NRP1		For 5'-AAAACGGTGCCATCCCT-3' Rev 5'-AAGAAGCAGAGTGGGTCGTT-3'
BIRC5		For 5'-TGAGAACGAGCCAGACTTGG-3' Rev 5'-TGTTCCTCTATGGGGTCGTCA-3'
KLF5		For 5′-GATCTAGATATGCCCAGTTC-3′ Rev 5′-CAGCCTTCCCAGGTACACTTG-3′
MMP7		For 5′-GAGTGAGCTACAGTGGGAACA-3′ Rev 5′-CTATGACGCGGGAGTTTAACAT-3′
JAG1		For 5'-CAAACACCAGCAGAAAGCCC-3' Rev 5'-TAAGTCAGCAACGGCCTCAG-3'
PTCH1		For 5'-ACAACAGGCAGTGGAAATTGGAAC-3' Rev 5'-CCCAGAAGCAGTCCAAAGGTGTAA-3'
Housekeeping genes	ACTB	For 5’- CCACCGCGAGAAGATGA-3' Rev 5'-CCAGAGGCGTACAGGGATAG-3'
	B2M	For 5'-GTCTTTCAGCAAGGACTGGTC-3' Rev 5'-CAAATGCGGCATCTTCAAACC-3'

Table S5: Antibodies

Target	Clone	Species	Dilution	Cat No.	Company
PTK7	31G9	Rat	1:2000	In house	
βcatenin	E-5	Ms	1:1000	Sc-7963	Santa Cruz
CyclinA2	BF683	mS	1:2000	CST4656	Cell Signaling Technology
CyclinD1	92G2	Rb	1:1000	CST2978	Cell Signaling Technology
CyclinE2	Polyclonal	Rb	1:1000	CST4132	Cell Signaling Technology
CDK2	78B2	Rb	1:1000	CST2546	Cell Signaling Technology
CDK4	D9G3E	Rb	1:1000	CST12790	Cell Signaling Technology
CDK6	DCS83	Ms	1:2000	CST3136	Cell Signaling Technology
p21	12D1	Rb	1:1000	CST2947	Cell Signaling Technology
P27	D69C12	Rb	1:1000	CST3686	Cell Signaling Technology
HSP70	W27	Ms	1:1000	SC-24	Santa Cruz
Tubulin	B-5-1-2	Ms	1:1000	T6074	Sigma Aldrich

IV. REFERENCES

(1) Bosc, N.; Muller, C.; Hoffer, L.; Lagorce, D.; Bourg, S.; Derviaux, C.; Gourdel, M.-E.; Rain, J.-C.; Miller, T. W.; Villoutreix, B. O.; Miteva, M. A.; Bonnet, P.; Morelli, X.; Sperandio, O.; Roche, P. Fr-PPIChem: An Academic Compound Library Dedicated to Protein-Protein Interactions. *ACS Chem. Biol.* **2020**, *15* (6), 1566–1574. https://doi.org/10.1021/acschembio.0c00179.

(2) El Turk, F.; Fauvet, B.; Ouertatani-Sakouhi, H.; Lugari, A.; Betzi, S.; Roche, P.; Morelli, X.; Lashuel, H. A. An Integrative in Silico Methodology for the Identification of Modulators of Macrophage Migration Inhibitory Factor (MIF) Tautomerase Activity. *Bioorg. Med. Chem.* **2010**, *18* (14), 5425–5440. https://doi.org/10.1016/j.bmc.2010.05.010.

(3) Sheetz, J. B.; Mathea, S.; Karvonen, H.; Malhotra, K.; Chatterjee, D.; Niininen, W.; Perttilä, R.; Preuss, F.; Suresh, K.; Stayrook, S. E.; Tsutsui, Y.; Radhakrishnan, R.; Ungureanu, D.; Knapp, S.; Lemmon, M. A. Structural Insights into Pseudokinase Domains of Receptor Tyrosine Kinases. *Mol. Cell* **2020**, *79* (3), 390-405.e7. https://doi.org/10.1016/j.molcel.2020.06.018.

(4) Le Guilloux, V.; Schmidtke, P.; Tuffery, P. Fpocket: An Open Source Platform for Ligand Pocket Detection. *BMC Bioinformatics* **2009**, *10*, 168. https://doi.org/10.1186/1471-2105-10-168.

(5) Schmidtke, P.; Bidon-Chanal, A.; Luque, F. J.; Barril, X. MDpocket: Open-Source Cavity Detection and Characterization on Molecular Dynamics Trajectories. *Bioinforma. Oxf. Engl.* **2011**, *27* (23), 3276–3285. https://doi.org/10.1093/bioinformatics/btr550.

(6) Korb, O.; Stützle, T.; Exner, T. E. Empirical Scoring Functions for Advanced Protein-Ligand Docking with PLANTS. *J. Chem. Inf. Model.* **2009**, *49* (1), 84–96. https://doi.org/10.1021/ci800298z.

(7) Wolber, G.; Langer, T. LigandScout: 3-D Pharmacophores Derived from Protein-Bound Ligands and Their Use as Virtual Screening Filters. *J. Chem. Inf. Model.* **2005**, *45* (1), 160–169. https://doi.org/10.1021/ci049885e.

(8) Lepourcelet, M.; Chen, Y.-N. P.; France, D. S.; Wang, H.; Crews, P.; Petersen, F.; Bruseo, C.; Wood, A. W.; Shivdasani, R. A. Small-Molecule Antagonists of the Oncogenic Tcf/Beta-Catenin Protein Complex. *Cancer Cell* **2004**, *5* (1), 91–102. https://doi.org/10.1016/s1535-6108(03)00334-9.

(9) Fang, L.; Zhu, Q.; Neuenschwander, M.; Specker, E.; Wulf-Goldenberg, A.; Weis, W. I.; von Kries, J. P.; Birchmeier, W. A Small-Molecule Antagonist of the β-Catenin/TCF4 Interaction Blocks the Self-Renewal of Cancer Stem Cells and Suppresses Tumorigenesis. *Cancer Res.* **2016**, *76* (4), 891–901. https://doi.org/10.1158/0008-5472.CAN-15-1519.

(10) Gonsalves, F. C.; Klein, K.; Carson, B. B.; Katz, S.; Ekas, L. A.; Evans, S.; Nagourney, R.; Cardozo, T.; Brown, A. M. C.; DasGupta, R. An RNAi-Based Chemical Genetic Screen Identifies Three Small-Molecule Inhibitors of the Wnt/Wingless Signaling Pathway. *Proc. Natl. Acad. Sci. U. S. A.* **2011**, *108* (15), 5954–5963. https://doi.org/10.1073/pnas.1017496108.

(11) Zhang, M.; Catrow, J. L.; Ji, H. High-Throughput Selectivity Assays for Small-Molecule Inhibitors of β-Catenin/T-Cell Factor Protein-Protein Interactions. *ACS Med. Chem. Lett.* **2013**, *4* (2), 306–311. https://doi.org/10.1021/ml300367f.

(12) Trosset, J.-Y.; Dalvit, C.; Knapp, S.; Fasolini, M.; Veronesi, M.; Mantegani, S.; Gianellini, L. M.; Catana, C.; Sundström, M.; Stouten, P. F. W.; Moll, J. K. Inhibition of Protein-Protein Interactions: The

Discovery of Druglike Beta-Catenin Inhibitors by Combining Virtual and Biophysical Screening. *Proteins* **2006**, *64* (1), 60–67. https://doi.org/10.1002/prot.20955.